Chemical Geology 644 (2024) 121842

Contents lists available at ScienceDirect

Chemical Geology

journal homepage: www.elsevier.com/locate/chemgeo

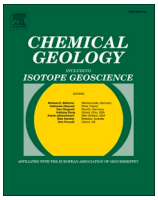

# Ikaite formation in streams affected by steel waste leachate: First report and potential impact on contaminant dynamics

Laura Bastianini [a,*], Mike Rogerson [b], Alex Brasier [c], Timothy J. Prior [d], Kit Hardman [e], Eddie Dempsey [f], Anna Bird [f], William M. Mayes [f]

[a] School of Engineering and Physical Sciences, Heriot-Watt University, Edinburgh EH14 4AS, UK
[b] Department of Geography and Environmental Science, Northumbria University, Newcastle, UK
[c] University of Aberdeen, School of Geosciences, Meston Building, Old Aberdeen, Aberdeen AB24 3UE, UK
[d] Department of Chemistry and Biochemistry, Faculty of Science and Engineering, University of Hull, Hull, UK
[e] Department for Science, Innovation and Technology, 100 Parliament Street, London SW1A 2BQ, UK
[f] Department of Geography, Geology and Environment, Faculty of Science and Engineering, University of Hull, Hull, UK

ARTICLE INFO

Editor: Claudia Romano

*Keywords:*
Ikaite
Alkaline sites
Carbonate systems
Carbon capture
Trace metal dynamics

ABSTRACT

Highly alkaline (pH 9–12) waters can arise from a range of globally significant and environmentally impactful industrial processes such as lime, steel and cement production, alumina refining and energy generation (e.g. combustion ashes). Such residue storage sites are often characterized by extreme geochemical conditions that can be hazardous to aquatic life but are quickly becoming a critical focus for resource recovery and carbon capture initiatives. The very high rates of mineral precipitation at these sites can give rise to the formation of transient minerals that are not currently well understood. As such our estimates of carbon budgets and understanding of trace metal dynamics at highly alkaline sites is currently limited. This study provides a significant advancement in the basis for characterising hyperalkaline carbonate systems through identification and chemical analysis of transient minerals forming in sites receiving high pH (>11) steel slag leachate in northern England. Whilst most of the secondary deposits at the study sites appear to be dominated by calcite, this study provides the first account of ikaite ($CaCO_3.6H_2O$) crystallization within steel-slag leachate, using novel field (Fourier Transform Infra-Red) supported by rapid laboratory (X-Ray Diffraction) validation. This study suggests that ikaite is a secondary mineral with a primary phase being amorphous calcium carbonate (ACC). Trace element analysis of ikaite forming in these steel-slag leachate affected waters is demonstrates its strong affinity to incorporate relatively large inventories of potentially harmful metals (e.g. lead and cadmium). Importantly, ikaite is only stable at low temperatures (−4 to 8 °C) and thus is of significant concern given its potential to release hazardous pulses of contamination during warming events in the spring. The findings provide an improved understanding of carbonate precipitation processes at highly alkaline sites which in turn should influence future research endeavours around mineral carbonation, trace metal dynamics and environmental remediation at these sites globally.

## 1. Introduction

Ikaite, calcium carbonate hexahydrate ($CaCO_3{\cdot}6H_2O$), is a rarely-reported hydrous calcium carbonate mineral forming by precipitation from strongly supersaturated, at least marine salinity solutions (Brooks et al., 1950; Pauly, 1963). As a consequence of its limited conditions of formation and its thermal instability, this mineral is poorly documented worldwide. Since ikaite was reported by Pauly (1963) forming at the bottom of Ikka Fjord in Greenland where cold (3 °C) carbonate-rich submarine springs mixed with seawater, recent ikaite has been reported in the SCOPUS database from <20 locations worldwide, including inference of its presence from pseudomorphs and cavities. Glendonites, which are considered to be pseudomorphs after calcite, are used in paleoclimate and sedimentology studies to reveal past cold-water environments, although their distribution is highly irregular in space and time. Rogov et al. (2021) provide an inventory of 700 occurrences of their associated carbonate pseudomorphs (glendonites) through the Phanerozoic. A significant body of evidence suggests that

* Corresponding author.
*E-mail address:* L.Bastianini@hw.ac.uk (L. Bastianini).

https://doi.org/10.1016/j.chemgeo.2023.121842
Received 17 October 2022; Received in revised form 18 October 2023; Accepted 18 November 2023
Available online 26 November 2023

glendonite occurrences are restricted to cold-water settings (Rogov et al., 2021), however they do not occur during every glaciation or cooling event of the Phanerozoic (Rogov et al., 2021). While Quaternary glendonites and ikaites have been described from all major ocean basins, older occurrences have a patchy distribution, which reflects poor preservation potential of both carbonate concretions and older sediments (Tollefsen et al., 2020).

### 1.1. Observations of recent ikaite

Glaring et al. (2015) returned to the submarine ikaite columns located in the Ikka Fjord in Southern Greenland to study the permanently cold (<6 °C) and alkaline (above pH 10) habitat of a microbial community adapted to these extreme conditions where ikaite was first reported. In their study, the function of abundant groups of bacteria in the ikaite columns is unknown, but alkaliphiles, corresponding to obligate methylotrophs common in soda lake environments, may potentially participate in carbon cycling in the ikaite columns by degrading the products of the heterotrophic anaerobes (Glaring et al., 2015). In addition, sulphate-reducing bacteria (SRB) appear to play an important role in the sulfur cycle in soda lakes and several orders of obligate anaerobic SRB were identified in the ikaite column interior. Rysgaard et al. (2013) significantly extended the Arctic range of ikaite, by discovering crystals of it in sea ice forming from waters with similar properties to those found in the original cold springs, which are large springs where the spring water is cold (<6 °C) because the volume of water is too important to be adequately warmed. Ikaite crystals have since been observed to precipitate within an hour in frost flowers forming from young Arctic sea ice (Barber et al., 2014). Ikaite also occurs in the anoxic marine sediments of Bransfield Strait on the Antarctic shelf (Suess et al., 1982), in sediment cores recovered from the Nankai Trough south of Japan (Stein, 1986) and the central part of the Zaire deep-sea fan (Jansen et al., 1987). It has been recognised as the parent mineral for thinolite pseudomorphs at the Lahontan and Mono Lake basins in California (Shearman et al., 1989; Bischoff et al., 1993a). Larsen (1994) identified calcite pseudomorphs formed from ikaite in lacustrine strata and travertine in the Creede caldera of south-central Colorado, and a late Holocene hydrological study of Ohlendorf et al. (2014) show that carbonate crystals occurred in lacustrine sediments of Laguna Cha'ltel (south-eastern Argentina) indicating a *syn*- or post-depositional formation of ikaite.

Despite being commonly short-lived and difficult to analyse, the broad distribution of ikaite in ice and sediment at near-freezing temperatures means it can alter the behaviour of carbon and compatible ions within its environments of growth and alteration. It has been suggested that ikaite precipitation in sea ice may be critical in modifying the quantity of $CO_2$ dissolved in the surface ocean ($pCO_2$) (Rysgaard et al., 2013), providing a transient inventory of carbon which could either be retained if ikaite mostly dehydrates to calcite, or else released when the ice melts. As this carbon is released as $CO^{2-}_{3(aq)}$ rather than as $CO_{2(g)}$, an increase in total alkalinity has been observed during the summer where dissolution of ikaite crystals is actively occurring (Rysgaard et al., 2013). The pH increase induced by these processes allows surface water to absorb further $CO_2$, providing a little-known but potentially important sink for carbon at the high latitudes (Ibid). Ikaite may be important for understanding water and carbon cycles on cold rocky planets such as Mars due to the suitability of formation conditions, and present strategies for recognizing hydrous carbonates including ikaite in compact reconnaissance imaging spectrometer results (Harner and Gilmore, 2015). Ikaite has been reported to have formed during winter months in cold springs waters at Shiowakka, Hokkaido, Japan (Ito, 1996, 1998). Dempster and Jess (2015) reported the occurrence of metamorphic ikaite porphyroblasts during an ultralow- temperature metamorphism with an exceptionally low geothermal gradient in Dalradian calcareous slates and metadolostones of western Scotland.

In a ground-breaking exploration of anthropogenic environments, Boch et al. (2015) describe a similar cold-water process of ikaite formation in an Alpine stream affected by concrete leachates, which extends the observation of this form of calcium carbonate into environments altered by human activity. Within this occurrence, electric conductivity (EC) values ranged from 65 to 3050 $mS.cm^{-1}$ and sampling sites of the upstream and central sections revealed the overall highest pH (12.9) and EC values (3050 $mS.cm^{-1}$) in the beginning of the monitoring period during winter (January 2014). They note that dissolved trace metals in solution sequestered into ikaite during the winter would be released back into the stream during the spring thaw, which temporarily changes the hydrochemistry of the system. As the concrete-influenced site they report lacks toxic trace metals, the primary influence is on carbonate chemistry. However, they note that toxic ions were present and spring-time ikaite dissolution might result in release as a pulse to the severe detriment of local water quality. These authors note that there is a severe knowledge gap of what this impact would be, or where it would likely be found. Similarly, Milodowski et al. (2013) observed ikaite within a lime-leachate affected site in Derbyshire UK, and Field et al. (2017) observed cavities formed after ikaite within fast growing, hyperalkaline speleothems (forming in tunnels below lime spoil) nearby at Peak Dale, Derbyshire, UK. The anthropogenic niche for ikaite formation and the issue of spring-time toxic ion release highlighted by Boch et al. (2015) may therefore be geographically extensive.

### 1.2. Formation conditions of ikaite

Precipitation of ikaite occurs in aqueous solutions near freezing conditions (temperature range of ca. -4 to 8 °C; Boch et al., 2015), extending to negative temperature values where ionic strength is high enough to prevent freezing (down to −8 °C; Hu et al., 2014; Papadimitriou et al., 2014). Crystallization of ikaite is also enhanced by elevated pressure conditions (>3 kbar at 25 °C) (Marland, 1975; Shahar et al., 2005). However, even under favourable physical conditions, ikaite is characterized by a solubility higher than the anhydrous calcium carbonate polymorphs calcite, aragonite and vaterite (Brečević and Nielsen, 1993; Marion, 2001). These polymorphs are known to be inhibited by dissolved compounds such as magnesium, phosphate, sulfate and organic molecules, whereas the latter promote the nucleation of ikaite (Brooks et al., 1950; Bischoff et al., 1993; Niedermayr et al., 2013). Bischoff et al. (1993) has shown that ikaite is undersaturated at all temperatures in seawater and in alkaline lakes, but rapidly reaches saturation near 0 °C. Its precipitation in near-freezing marine sediments necessitates large additions of $HCO_{3(aq)}$ to pore fluids from the diagenetic decomposition of organic matter (Bischoff et al., 1993). However, its crystallization in tufas or alkalines lakes requires only small additions of Ca from springs (Bischoff et al., 1993). Kinetic experiments have demonstrated that ikaite is stabilized in natural environments by orthophosphate, which prevents the crystallization of the more stable anhydrous form $CaCO_3$ but does not interact with the ikaite (Bischoff et al., 1993). Microbial activity associated with anoxic conditions can also influence ikaite formation via recycling of organic compounds in marine sediments (Stougaard et al., 2002; Olcott et al., 2005), and microbial diversity is well developed in ikaite tufa columns in Greenland (Stougaard et al., 2002). This very alkaline (pH 10.4) and cold (4 °C) environment favour the development of a wide range of algae and metazoans (Buchardt et al., 1997; Kristiansen and Kristiansen, 1999) but also a diverse bacterial community, both in the column interior and at the surface, and very few archaea (Glaring et al., 2015). Biofilms on the surface of the columns, especially on newly formed ikaite material, is dominated by Cyanobacteria and phototrophic Proteobacteria, whereas Proteobacteria and putative anaerobic representatives of the *Firmicutes* and *Bacteroidetes* are concentred in the column interior (Glaring et al., 2015). It seems likely therefore that growth of ikaite is significantly favoured by the presence of biofilms, to the extent that growth of this mineral is rare without it. The mechanism is not yet determined but may relate to the role of organic molecules impeding the formation of anhydrous forms in a manner analogous to that already observed in phosphate.

Natural and anthropogenic environmental conditions where there is abundant $OH^{-}_{(aq)}$ may also favour the formation and rapid deposition of ikaite, using calcium directly from the dissolved Ca-OH reservoir (Boch et al., 2015):

$$Ca^{2} + (aq) + 2OH^{-}_{(aq)} + 5H_2O_{(l)} + CO2(g) \rightleftharpoons CaCO_3.6H_2O_{(s)} \quad (1)$$

Ikaite precipitated by the forward reaction when temperature is low enough for this to be favoured may dissolve again by the reverse reaction (although high pH likely results in the carbon being retained as $HCO^{-}_{3(aq)}$), or it may alter to calcite by dehydration.

$$CaCO_{(3)0}.6HO_{2(s)} \rightleftharpoons CaCO_{3(s)} + 6H_2O_{(l)} \quad (2)$$

The straightforward stoichiometry of 1 underlines why ikaite grows so freely where stream waters interact with concrete, or other systems where soluble cement phases such as portlandite ($Ca(OH)_{2(s)}$) are present. The discovery of pseudomorphs after ikaite in a railway tunnel affected both by concrete leaching and by impacts from surface tips of lime spoil in the UK (Field et al., 2017) gives a good example of the anthropogenic settings where ikaite has been documented. In such carbon-limited conditions such as streams affected by concrete leachates, whenever water temperature is low enough to favour ikaite formation, absorption of gaseous $CO_2$ into the alkaline solution and its hydroxylation with $OH^{-}$ are likely the rate-determining parameters (Boch et al., 2015).

Ikaite grows most generally in the natural environment below the sediment-water interface in continental shelf settings (e.g. Greinert and Derkachev, 2004; Lu et al., 2012; Zabel and Schulz, 2001; Zhou et al., 2015). High levels of bacterial sulphate reduction supported by high amounts of sedimentary organic matter or by anaerobic oxidation of methane (AOM) tend to enhance ikaite precipitation in such settings (Vickers et al., 2022).

Factors ensuring a sufficiently high supersaturation such as elevated alkalinity, alkaline solution conditions (Boch et al., 2015; Hu et al., 2015), and cold temperatures (Stockmann et al., 2018; Tollefsen et al., 2020) favour the formation of ikaite. Substances inhibiting calcite precipitation, typically aqueous $Mg^{2+}$ and phosphate can further support ikaite formation (Hu et al., 2014; Stockmann et al., 2018; Tollefsen et al., 2020). However, the presence of such substances is not necessary for ikaite formation as demonstrated by several experimental studies at cold solution temperatures (Besselink et al., 2017; Boch et al., 2015; Hu et al., 2015; Zou et al., 2018). The physicochemical conditions at the origin of ikaite rather than anhydrous carbonates are still unknown even though the number of studies on ikaite formation is important (Strohm et al., 2022). This is partly because conditions which enhance ikaite formation may induce a more rapid transformation of ikaite into more stable calcium carbonate minerals. Besselink et al. (2017) and Zou et al. (2018) have measured a start of ikaite precipitation during dissolution of a previously formed amorphous calcium carbonate precursor within experiments in highly supersaturated solutions but the amorphous precursor needs to be composed of an amount of water similar to ikaite (Zou et al., 2018)0.**1.3 | Crystallization of ikaite.**

Generally, anhydrous calcium carbonate (calcite, vaterite, or aragonite) occur as the dominant polymorphs throughout the natural environment, compared to hydrated (monohydrocalcite and ikaite), or amorphous forms (amorphous calcium carbonate: ACC) (Chaka, 2018), which need specific conditions to remain stable. Very rapid precipitation favours non-classical mechanisms, where kinetic rather than thermodynamic conditions regulate how the precipitate is assembled (Oaki and Imai, 2003; Power et al., 2014, 2017). In this situation, aqueous ions are hypothesized to condense into prenucleation clusters which retain the coordination of dissolved ions and aggregate to form ACC rather than thermodynamically favoured forms with more ordering (Chaka, 2018; Power et al., 2017). For the same reasons, highly hydrated structures such as ikaite, lansfordite, and nesquehonite would be expected to have a higher probability of kinetic formation, even if not thermodynamically favoured, due to the similar cation coordination in the solid and the solution (Chaka, 2018; Power et al., 2014, 2017). The hexahydrate ikaite structure is extensively hydrated with each Ca coordinated to six water molecules and one η2 carbonate group (Chaka, 2018). Demichelis et al. (2011) show this structure is stabilized by an extensive hydrogen bonding network. Formation of ikaite from amorphous prenucleation clusters may be promoted because the $Ca - O_{ikaite}$ ion distances are very similar to the distances in water. Modelled values for the ion distances in ikaite are 2.443 Å (Demichelis et al., 2011), which is in close agreement with measurements from synchrotron X-ray diffraction (Lennie et al., 2004) of 2.469 Å at 243 K and of 2.46 Å for 8-fold Ca coordination in an aqueous environment with large-scale X-ray scattering (Jalilehvand et al., 2001), compared to 2.490 Å for $Ca - O_{water}$ (Demichelis et al., 2011). Ikaite can therefore form directly from amorphous precursors, increasing its likelihood of formation where precipitation is rapid (Jalilehvand et al., 2001). In addition to similar ion distances between aqueous and ikaite Ca—O bonds, calcium coordination is also the same for ikaite and calcium carbonate in solution, and each carbonate ion is oriented in opposing directions to ensure a nonpolar structure (Gebauer et al., 2008; Montes-Hernandez and Renard, 2016). The dipoles are separated by 4.118 Å in both systems due to the coordinated waters in between, and provide an electrostatic driving force for alignment of the complexes in solution (Gebauer et al., 2008; Montes-Hernandez and Renard, 2016).

### *1.3. Transformation of ikaite to other calcium carbonate polymorphs post-deposition*

Monohydrocalcite and ikaite can crystallize from an initial product of ACC as well as precipitating directly. Similarly, ikaite has also been shown to transform to ACC, and subsequently to vaterite, if local conditions favour that sequence (Chaka, 2018). ACC is generally considered a hydrated form of Ca carbonate and has water content typically ranging from 0.5 to 1.4 mol of water per mole of $CaCO_3$, although biogenic ACC may have up to 15.25% (Chaka, 2018). The reaction in either direction occurs without a change in the coordination of the cation, and are kinetically efficient. Ikaite can thus be considered one possible point in an Ostwald Step Rule sequence, which may occur where kinetic controls regulate precipitation, or where additives within the solution inhibit thermodynamically favoured forms.

### *1.4. This study*

Here, we provide the first report of ikaite in a steel waste leachate environment, at 135 m altitude and at temperate latitude (54.51°N). This is significant, because there are a range of toxic metals and metalloids available in this system which may be accumulated in the ikaite inventory as it forms, concentrated and then released as the mineral transforms; there is therefore urgent need to close the knowledge gap identified by Boch et al. (2015). We use novel in-situ and laboratory experimental approaches to address the questions of which ions may be accumulated in transient ikaite inventories, and how this complicates understanding of pollutant dynamics in steel waste-affected sites worldwide.

## 2. Materials and methods

### *2.1. Field work*

#### *2.1.1. Description of the site*

In Howden Burn, calcite saturation is enhanced by four alkaline discharges within the former Consett Iron and Steelworks, County Durham, UK (54°51.2360′N; 1°51.7320′O). The site was operational from the middle of the Nineteenth Century until decommissioning in the early 1980's (Fig. 1). Waste up to 45 m depth, including slag, flue dusts, ashes and construction and demolition rubble were accumulated after

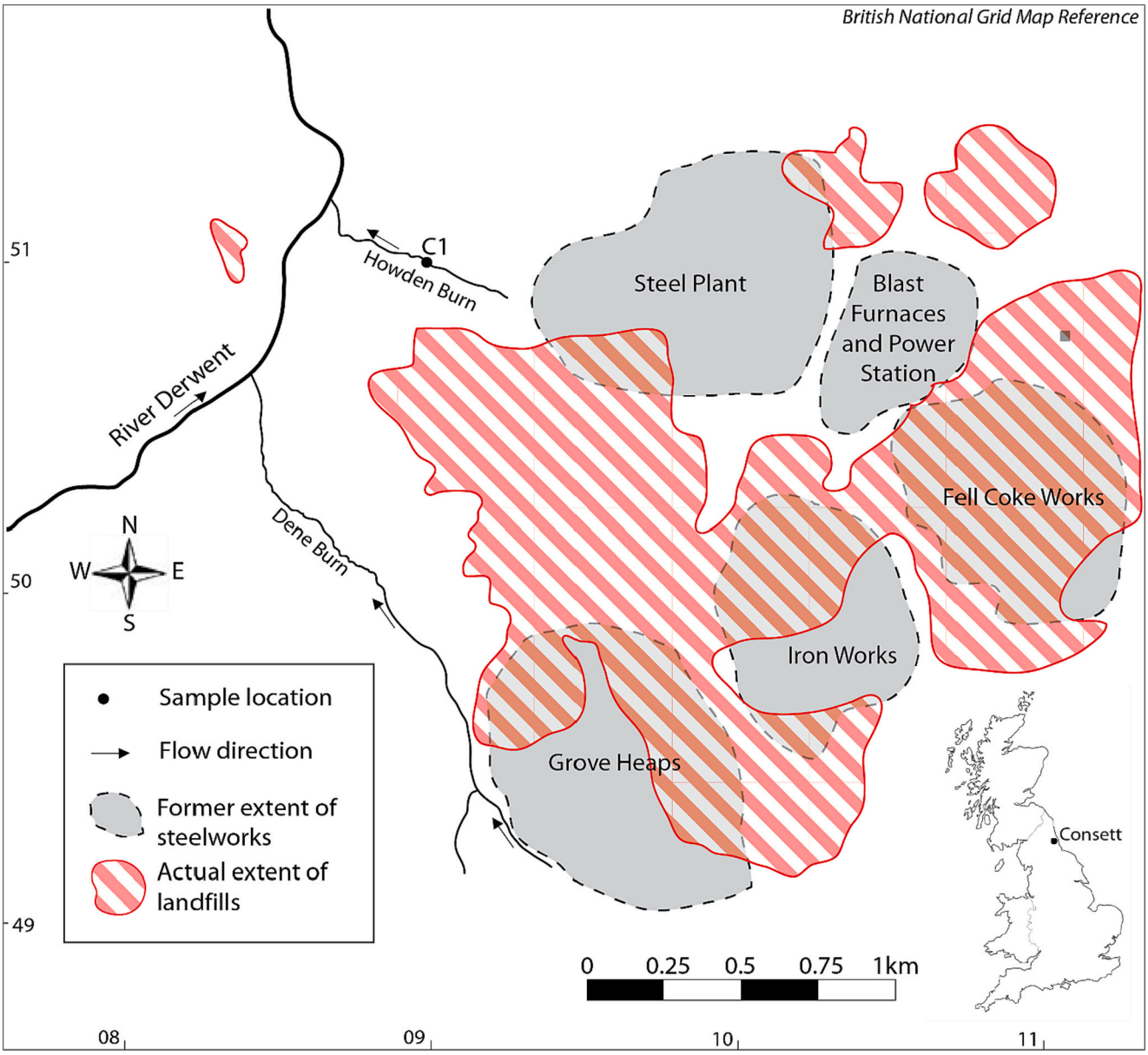


**Fig. 1.** Location map of the studied sample HU-MR-/3CON1 (C1).

working closure in an area of 2.9 $km^2$ (Harber and Forth, 2001). These materials are now stored in landfill, and the leachates emerging from them are alkaline ($[OH^-]$ = 10–130 $mg.L^{-1}$; $[CO_3^{2-}]$ = 10–110 mg.L-1; $[HCO_3^-]$ = 110 $mg.L^{-1}$) because of the bulk chemical composition meteoric waters develop after interacting with these materials in the subsurface (Mayes et al., 2008, 2018; Riley and Mayes, 2015). These landfills can be a source of pollution to surface and ground waters (Mayes et al., 2008; Fig. 1). Iron and steel flue dusts contain metals including boron, lead, cadmium, halide, fluoride, zinc, chromium, arsenic, copper, nickel, and alkali metals and coke making provides inorganic compounds such as zinc, fluoride, sulfate, phosphate and organic compounds from fuels and oils (Harber and Forth, 2001).

Howden Burn leachate sources are mixed waters rich in K, Na, Ca, and sulfate (Mayes et al., 2008) (Fig. 1). Sulfate concentrations are exceptionally elevated [2500 $mg.L^{-1}$] typical of a drainage from the former power station and coke works area of the workings (Fig. 1). Within these locations, coke works spoil, ashes, and iron slags, which have a high sulfur content, were co-deposited with steel and blast furnace slag (Harber and Forth, 2001). The very high potassium content of Howden Burn leachate sources probably derive from highly soluble potassium oxides associated with flue dusts and ashes deposited with slag (Mayes et al., 2008). The contaminants of most environmental concern are those potentially soluble at high pH, because they form oxyanions (e.g. As, Cr and *V*), which can be very mobile as they sorb weakly to soils and sediments (Cornelis et al., 2008; Mayes et al., 2011).

Alkalinity and high Ca content of emerging waters cause rapid carbonation in streams affected by the leachate, resulting in sediment deposits described by Bastianini et al., 2019, 2021. The deposit at Consett comprises a tufa barrage system, with barrages measuring 20 cm in height and predominantly composed of buff-coloured calcitic tufa carbonate.

### 2.1.2. *Strategy for finding ikaite*

White growths on the surface of the carbonate deposit had previously been observed when there was snow on the ground one week before collection of the sample (29th January 2019). Consequently, a sampling

team visited the site later during the same cold period (average air temperature of 0.9 °C on 30th January 2019, −4.35 °C on 3rd February 2019 and 1.1 °C on 5th February 2019 after CEDA Archive from the nearest station of Durham) (Fig. 2).

The sampling team looked for crystalline growths not present in warm weather, focussing on the previously reported scattering of cm-sized euhedral to subhedral white grainy crystals (Fig. 3), which were suspected ikaite. Rising above (and apparently cemented to) the buff-coloured tufa carbonate during this visit were such a scattering of cm-sized euhedral to subhedral white crystals, dominantly located along the barrage crests (Fig. 3). The sampled carbonate precipitate described here is a white crystalline material which exhibits a grainy consistency (Fig. 3) taken from one of these growths. All these precipitates formed within a few days only, and such precipitates are not found at the site outside of similar very brief spells of unusually cold weather.

#### 2.1.3. Collection of the sample

The sample (HU-MR-/3CON1 — C1) was taken on 5th February 2019 along a pre-established calcite saturation index transect (Mayes et al., 2008, 2018; Riley and Mayes, 2015) within Howden Burn (Fig. 1). This sample was recovered with a sieve to prevent heating by contact with skin and handled by plastic tweezer (Fig. 4). Initial identification was by ATR-Fourier Transform Infrared (FTIR) spectroscopy using a portable Agilent 4300 Portable FTIR immediately after sampling and sample air drying on the stream bank to avoid water interference on FTIR. This innovative approach minimised the risk of alteration of ikaite crystals after sampling, and we are not aware of this approach being previously used. The peaks were analysed and characterized by the MicroLab FTIR Agilent Software.

During our sampling, on-site measurements of major physico-chemical parameters (pH, electrical conductivity and water temperature) were performed using a Myron L Ultrameter® calibrated with pH 4, 7 and 10 buffer solutions and a 1413 μS conductivity standard, to confirm the system had not changed since previous sampling.

### 2.2. XRD

The sample of ikaite recovered by the sampling team at Consett was air dried on site and transported under ice. On return to the laboratory, it was immediately analysed (within 6 h of sample collection) using a very long collection of single crystal XRD. During laboratory investigation, the sample was stored over dry ice. A small portion of the sample was removed from the sample bag and placed under a microscope. A portion of this, representative of the bulk, was rapidly mounted at the end of a glass fibre on a goniometer and the sample transferred into a nitrogen gas cryostream at 250 K. The sample was examined by X-ray diffraction; a Weissenberg image was recorded while the sample was rotated about ϕ. This pattern (Fig. S1) did not show the presence of dominant rings characteristic of a powder, but a highly symmetric arrangement of spots consistent with a single crystal. The complete hemisphere of data was therefore collected from this crystal sample.

Diffraction data were collected using a Stoe IPDS2 image plate diffractometer operating with Mo radiation at the department of Chemistry and Biochemistry, University of Hull, UK. A full hemisphere of diffraction data were collected in a series of omega scans (180 × 1°) with a 120 s exposure time. The data were scaled, merged, and corrected for absorption using the program Sortav. Non-hydrogen atoms were refined using the published positions as the starting model and hydrogen atoms of water were identified from difference Fourier maps and placed subject to chemically-sensible restraints on bond lengths and angles. The program SHELXL-2018 was utilised for least squares refinement of the crystal structure (Sheldrick, 2015).

### 2.3. Microscopy

To identify the micro-texture and the micro-scale fabrics, a Cryo-Scanning Electron Microscope (Zeiss EVO 60) attached to an EDS detector (Oxford Instruments INCA System350 with Silicon Drift Detector) was used at the Department of Chemistry and Biochemistry, University of Hull.

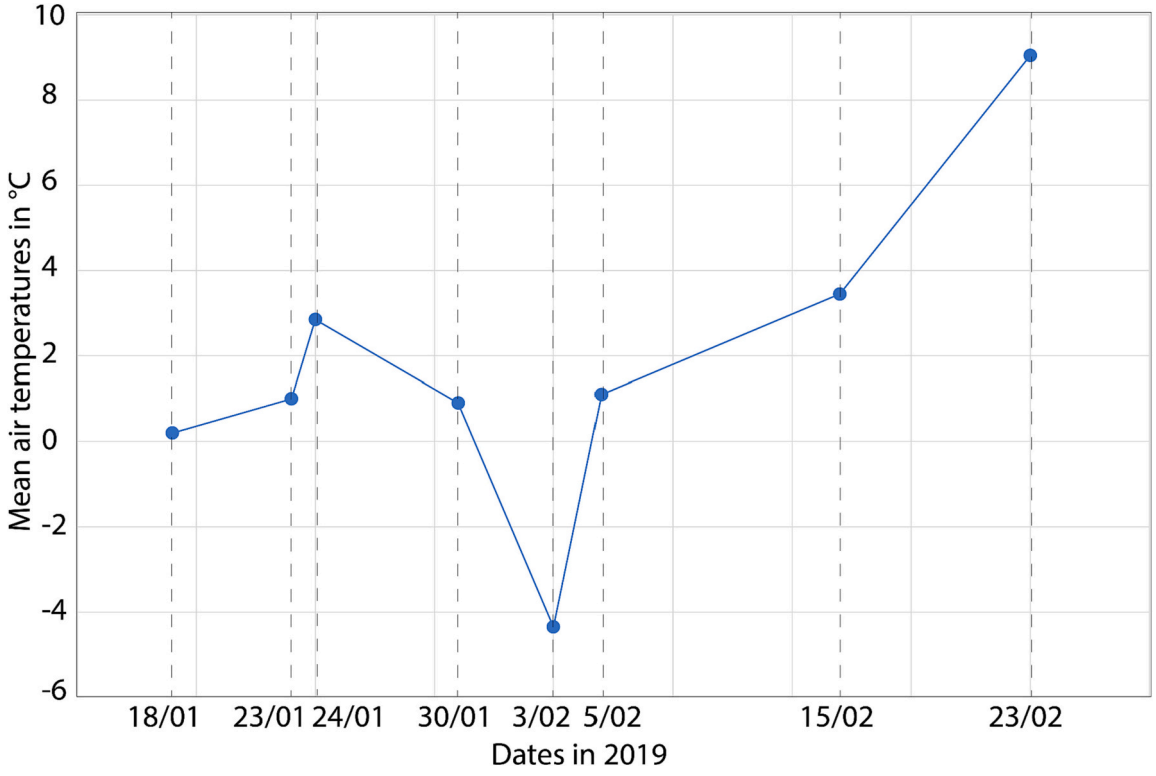


**Fig. 2.** Graph depicting the average air temperatures in Durham versus the dates after CEDA Archive (sample collection date: 5/02/2019).

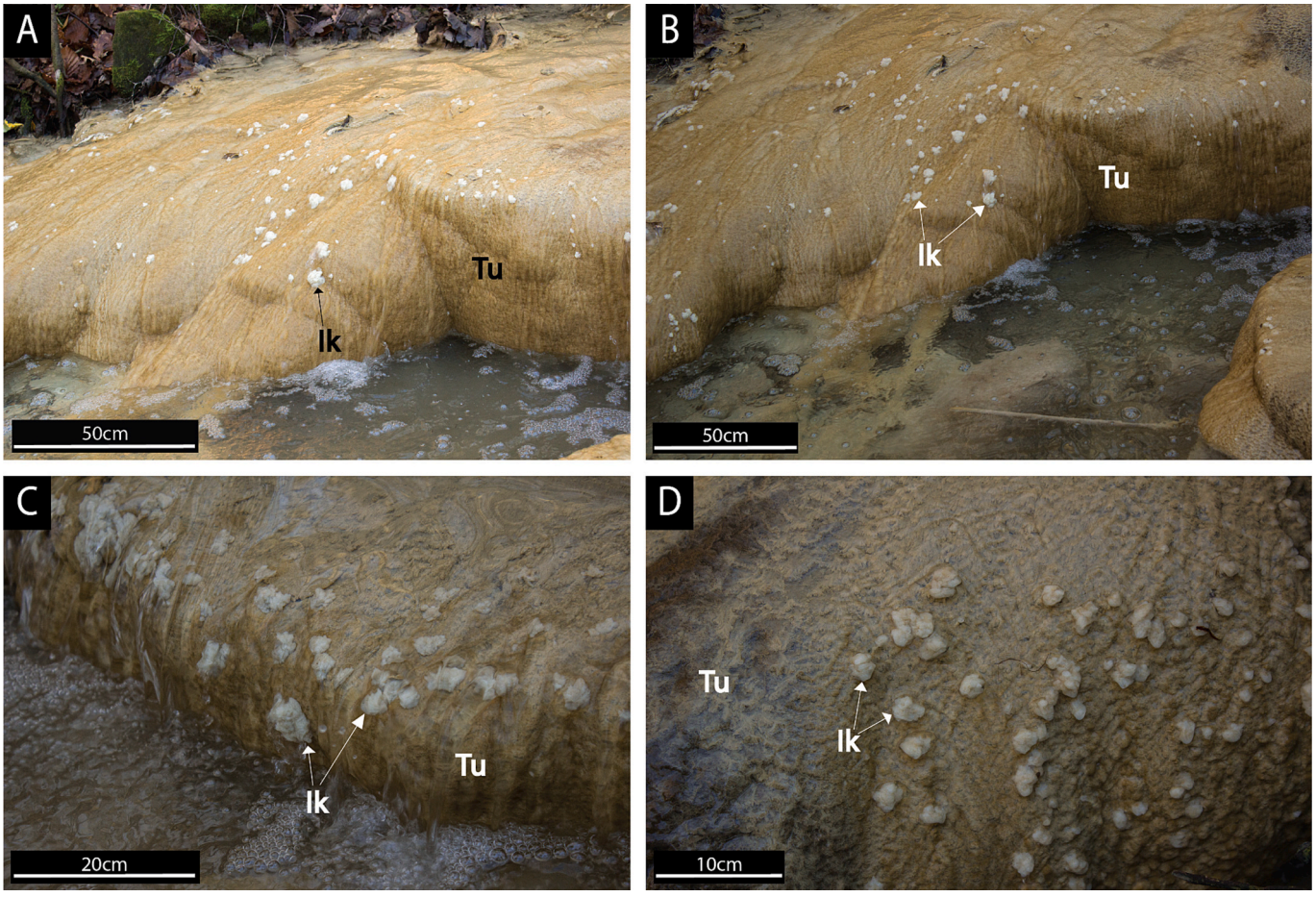


**Fig. 3.** Macroscopic images of the Consett freshwater sample HU-MR-/3CON1 depicting a scattering of cm-sized euhedral to subhedral white crystals of ikaite (Ik) rising above and cemented to the buff-coloured orange-red oxidated tufa carbonate (Tu). (For interpretation of the references to colour in this figure legend, the reader is referred to the web version of this article.)

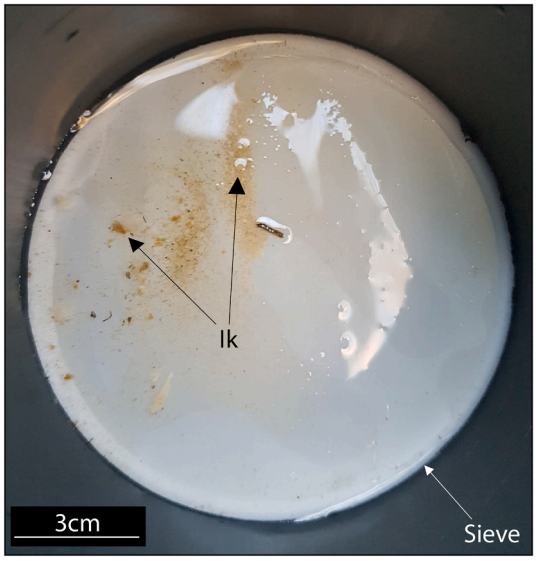


**Fig. 4.** Recovered sample of ikaite (Ik) within the sieve.

### 2.4. Trace Element content

Table 1 illustrates the different data which are characteristic for the method used (LA-ICP-MS). This table is divided into four sections – laboratory and sample preparation, information about the laser ablation system, information about the ICP-MS instrument, and details of the data processing approach. In this method, we used the idealised formula for ikaite to provide the mass fraction for calcium, and the data are normalised to CaCO3 which is around 50% ikaite in idealised ikaite using values from (Hiruta and Matsumoto, 2022).

Trace element partition coefficients, $Kd_X$, were calculated from the data using:

$$Kd_X == \frac{X_{Solid}/Ca_{Solid}}{X_{Solution}/Ca_{Solution}}$$

where $X_{Solid}$ represents the concentration of a certain trace element in the studied sample of ikaite, $X_{Solution}$ represents the concentration of a certain trace element in the solution (as we do not know precisely when the crystal grew, we use long-term average data of trace element concentrations in the fluids from the site; Hull et al., 2014; Riley and Mayes, 2015; Gomes et al., 2018; Bastianini et al., 2019), $Ca_{Solid}$ is the concentration of calcium in the studied sample of ikaite determined by LA-ICP-MS.

## 3. Results

### 3.1. Mineralogy

The FTIR spectra of the sample immediately after collection showed absorptions at 718, 1485, and 3182 $cm^{-1}$ (Fig. 5), which we compare to reported absorptions in calcium carbonate polymorphs (Table 2). The

**Table 1**
Reporting template (metadata) for LA-ICP-MS U-(Th-)Pb data.

| Laboratory and Sample preparation | |
|---|---|
| Laboratory name | Geography, Geology and Environment (University of Hull) |
| Sample type/ mineral | Ikaite grains, mounted on milled puck |
| Sample preparation | Grain mounting |
| Imaging | None |
| | |
| Laser ablation system | |
| Make, Model and Type | Applied Spectra, RESOlution-SE 193 nm |
| Ablation cell and volume | Laurin Technic S155 two volume cell |
| Laser wavelength | 193 nm |
| Pulse width | 5 ns |
| Fluence | 5 J.cm$^{-1}$ |
| Repetition rate | 20 Hz |
| Ablation duration | Scan length dependent |
| Spot diameter | 100 μm |
| Sample mode/ pattern | Line scans |
| Scan Speed | 0.005 mm.s$^{-1}$ |
| Carrier gas | He + $N_2$ in the cell, Ar carrier gas to torch |
| | |
| ICP-MS Instrument | |
| Make, Model and Type | Agilent 8800 |
| Sample introduction | Ablation aerosol mixed with Ar and sent to ICP-MS |
| RE power | 1170 W |
| Nebuliser gas flow | Ar 0.80 l.min$^{-1}$ |
| Detection system | Electron multiplier in counts per second mode |
| Masses measured | 9, 10, 25, 27, 31, 43, 45, 50, 53, 55, 59, 60, 65, 66, 87, 89, 103, 110, 124, 135, 206 |
| Integration time | 9, 10, 45, 53, 59, 60, 66, 89, 103, 110, 124 = 0.1 s; 135, 206 = 0.05 s; 25, 87 = 0.002; 43, 50 = 0.02; 27 = 0.001; 31 = 0.025; 55 = 0.004; 65 = 0.0333 |
| | |
| Data Processing | |
| Calibration strategy | 612 used as primary reference material, 610 used as secondary for validation |
| Internal Reference | Ca43 semiquant |
| Data processing package | Iolite v4, Data Reduction Scheme – Standard Trace Elements – quantitative (Longerich et al., 1996) |

latter peak is typical of O—H stretching, and as the sample was carefully air-dried before analysis indicates the presence of abundant formation water. The shape of the absorption peak for formation water is also less broad than free water, and has characteristic asymmetry and triple-peak structure so this water is certainly bound within the mineral. Absorption at 1485 cm$^{-1}$ reflects asymmetric $CO_3$ stretching (Gunasekaran et al., 2006), albeit with a small instrument-specific translation from the typical calcite absorption at ~1450 cm$^{-1}$ (Ibid). Absorption at 718 cm$^{-1}$ is symmetric $CO_3$ deformation, which is correct for ikaite but is not reported from ACC and is present at lower wavenumber in monohydrocalcite.

A white crystalline block of size 0.38 × 0.30 × 0.28 mm$^3$ was transferred to the single crystal diffractometer and held at 250 K in a nitrogen gas cryostream. This pattern did not show the presence of rings characteristic of a powder, but a highly symmetric arrangement of spots consistent with a single crystal. The complete hemisphere of data was therefore collected from this crystal sample.

The sample examined was dominated by crystalline domain of ikaite, but there were other much smaller crystals present. Spots from several other domains (at least 4 domains) were present in diffraction images, but it was possible to integrate the data for the dominant phase without problems (Fig. S2). The $R_{int}$ value of 0.0263 confirms the excellent consistency of data from this domain. It was not possible to identify other phases using the raw diffraction images, but a simulated powder diffraction pattern (Intensity v. 2θ) produced from the Weissenberg image shows the presence of minor calcite in the block examined (Fig. 6).

Diffraction data from the single dominant domain were integrated using standard procedures. The structure of ikaite ($CaCO_3.6H_2O$) was refined against these data and this unequivocally confirms that ikaite is the dominant component. The structure obtained is in good agreement with earlier structure determinations. The coordination about the calcium ion is shown in Fig. 7. The diffraction data and structure have been deposited at the CCDC and are available free of charge from ccdc.cam.ac.uk/structures with the REFcode *VIXQEB* (1902435).

### 3.2. SEM

SEM images (Figs. 8A-F) illustrate the shape of crystals from the carbonate crusts. Crystal sizes range from 10 nm to 5 μm (Figs. 8 A-E).

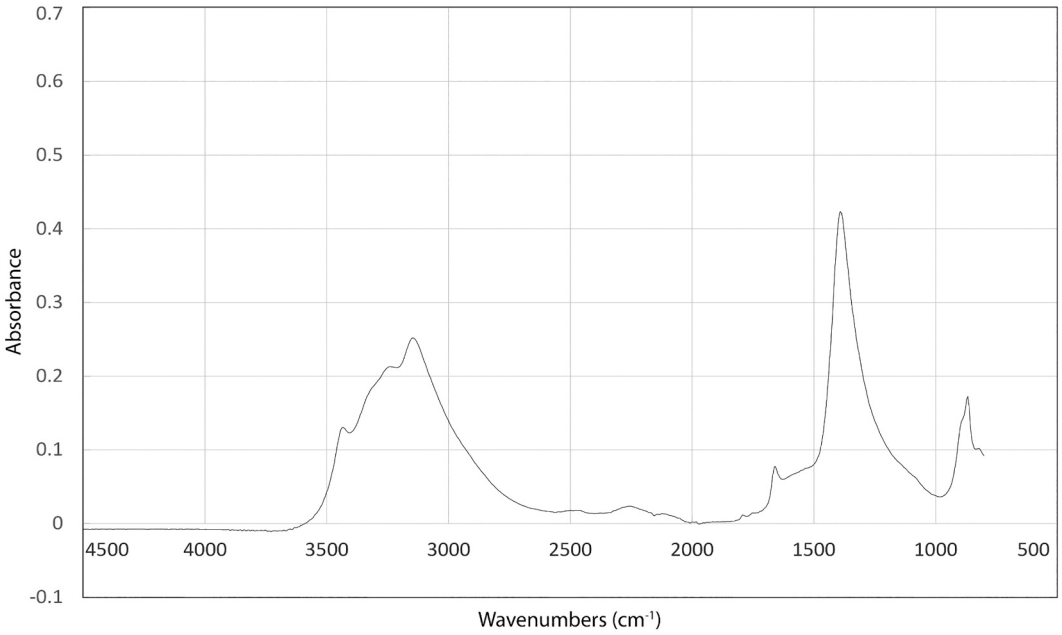


**Fig. 5.** FTIR spectra of the sample of ikaite C1.

**Table 2**
FTIR review with the different peak diagnostic of the $CaCO_3$ polymorphs.

| Wavenumber in $cm^{-1}$ | | | | | | |
|---|---|---|---|---|---|---|
| Reference | Calcite | Aragonite | Vaterite | ACC | Ikaite | Monohydrocalcite |
| Xyla and Koutsoukos, 1989 | 714/848/876/1800 | 842/857/1080 | 714/745/848/857/1070 | | | |
| Gauldie et al., 1997 | | 701/1085 | 713/1066 | | | |
| Chakrabarty and Mahapatra, 1999 | 713/874 | 700/712/844/874/1083 | 744/844/854/876/1087 | | | |
| Mikkelsen et al., 1999 | 712/1086/1436 | 705/854/1086 | 738/750/1077/1090 | | 719/1070 | |
| Kontoyannis and Vagenas, 2000 | 711/1085/1435 | 700/705/1084/1085 | 738/750/1074/1084/1089 | | 718/1070/3120/3270/3434 | |
| Tlili et al., 2002 | | | | | 722/873/1072/1485/3182/3240/3425 | |
| Coleyshaw et al., 2003 | | | | | 720/743/1411/1425/3119 | 580/698/762/872/1063/1401/1492/3236/3327/3400 |
| Carteret et al., 2009 | 712/1086 | 701/1085/1431/1531 | 1075 | | | |
| Qu et al., 2017 | 712/1086 | 701/1085 | 1075 | | | |
| Rodriguez-Blanco et al., 2011 | 725/874/1090/1409/1805 | | | 1460/1645 | | |
| Zhang et al., 2012 | 713/875/1420 | 700/713/856/875/1440/1490 | 745/875/1440/1490 | 866/1418/1475 | | 700/875/1408/1487 |

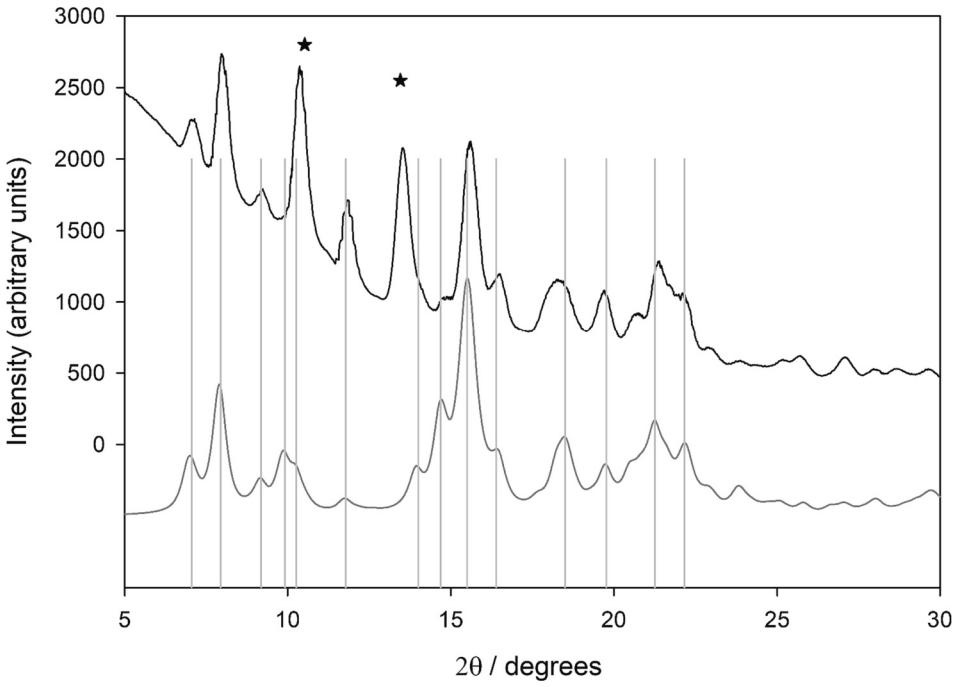


**Fig. 6.** One-dimensional diffraction pattern collected from HU-MR-/3CON1 crystallite (solid black line). The grey line is the simulated pattern for ikaite (with peak positions highlighted as vertical lines). The two starred peaks correspond to calcite.

Figs. 8A-B depict smooth surfaces, which have ridges running in straight lines that are quite parallel to the faces on the larger crystal. A striking feature observed is the sigmoidal bending of crystal faces ("s-like"; Fig. 8F). The SEM images (Fig. 8D) show that the morphologies of these white crystals are consistent with those of monoclinic ikaite (cf. Demichelis et al., 2014), and observed dimensions and habits are equivalent to those reported by other studies (Bischoff et al., 1993; Ito, 1996; Omelon et al., 2001; Dieckmann et al., 2008; Rysgaard et al., 2012). However, there are some interesting differences between the crystals observed under the electron microscope in this study and those observed elsewhere. First, most earlier studies have illustrated pitted crystals that have apparently partially transformed into calcite (e.g. Fig. 6A and D of Ito, 1996; Fig. 2 of Tollefsen et al., 2020). This pitting is not evident in crystals we have examined, perhaps because the crystals were kept cold and imaged as soon as possible in a cryoSEM. Rather, Fig. 8 shows ikaite crystals in which some smooth faces are well developed, but there are clearly some stepped and kinked faces that are less favoured and less well developed. This stepping of some faces could either be the result of incomplete growth, or of partial dissolution (Snyder and Doherty, 2007).

The ridges running parallel to the best developed crystal faces (blue lines on Fig. 8) could plausibly be interpreted as aligned crystal terminations (c-axis) of numerous small nucleating ikaite crystals. This would be analogous to 'feather crystals' of hot-spring travertines, which align with their tips normal to the substrate to form 'micro-terracette' ridges on sloping surfaces, oriented perpendicular to the direction of flow of a thin film of (aragonite or calcite-precipitating) water (Gandin and Capezzuoli, 2014). That the ridges of Fig. 8A-8B are aligned parallel to

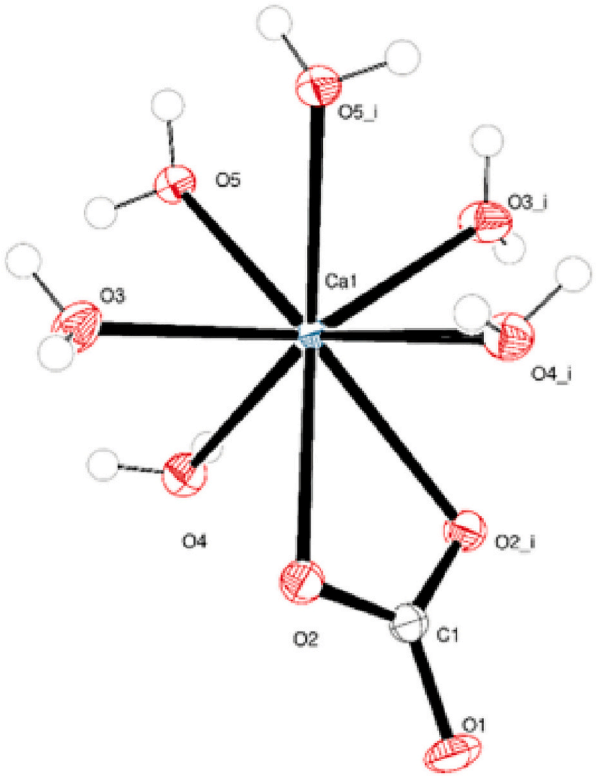


**Fig. 7.** Coordination about the Ca2+ ion with atoms shown as 50% probability ellipsoids. Atoms labelled name i are generated by the symmetry operator $i = 1 - x, y, ½ - z$.

the favoured faces of larger crystals suggests the stepped and kinked faces of the associated larger crystals (Fig. 8D-E) are likely also reflecting incomplete growth here, rather than dissolution following completed crystal development.

### 3.3. Laser ablation ICP-MS

Vanadium, chromium, nickel, zinc, cadmium and barium elements are present in trace amounts (median average concentration 0.001–0.17 mMol.Mol$^{-1}$), whereas manganese, copper and lead are two orders of magnitude more abundant (3.1–7.5 mMol.Mol$^{-1}$), and Sr is three orders of magnitude more abundant [81.4 mMol.Mol$^{-1}$]. In terms of dispersion, V, Cr, Mn, Ni, Zn, Cd and Ba attest of a low relative standard deviation lower than 1 [0.0009–0.16] but Cu, Sr and Pb have high relative standard deviation [26.7–71.19], which indicates variable content of these trace elements.

The trace element partition coefficients for the sample of ikaite are listed in the Table 3. All the partition coefficients are much higher than the range of partition coefficients for calcite and aragonite.The partition coefficients for ikaite of Cu, Cd, Cr, Mn, and Ni are 100 times higher than those of calcite, whereas Ba and Zn present a partition coefficient 1000 times higher, Pb 10,000 times higher and Sr 1000,000 times higher in order of magnitude.

### 3.4. Laboratory experiments

Figs. 9 and 10 show the FTIR spectra of the trials of making ikaite from the methods of Lennie et al. (2004) and Tollefsen et al. (2020) respectively. These spectra are diagnostic of ACC via four characteristic features (Figs. 9 and 10): a broad band between 2700 and 3600 cm$^{-1}$ (O—H stretching), a shaper band at 1650 cm$^{-1}$ (O—H bending), both of which correspond to structural water within ACC, a shoulder on the main asymmetric $\nu$3 CO3 band (at 1460 cm$^{-1}$) and the absence of the $\nu$4

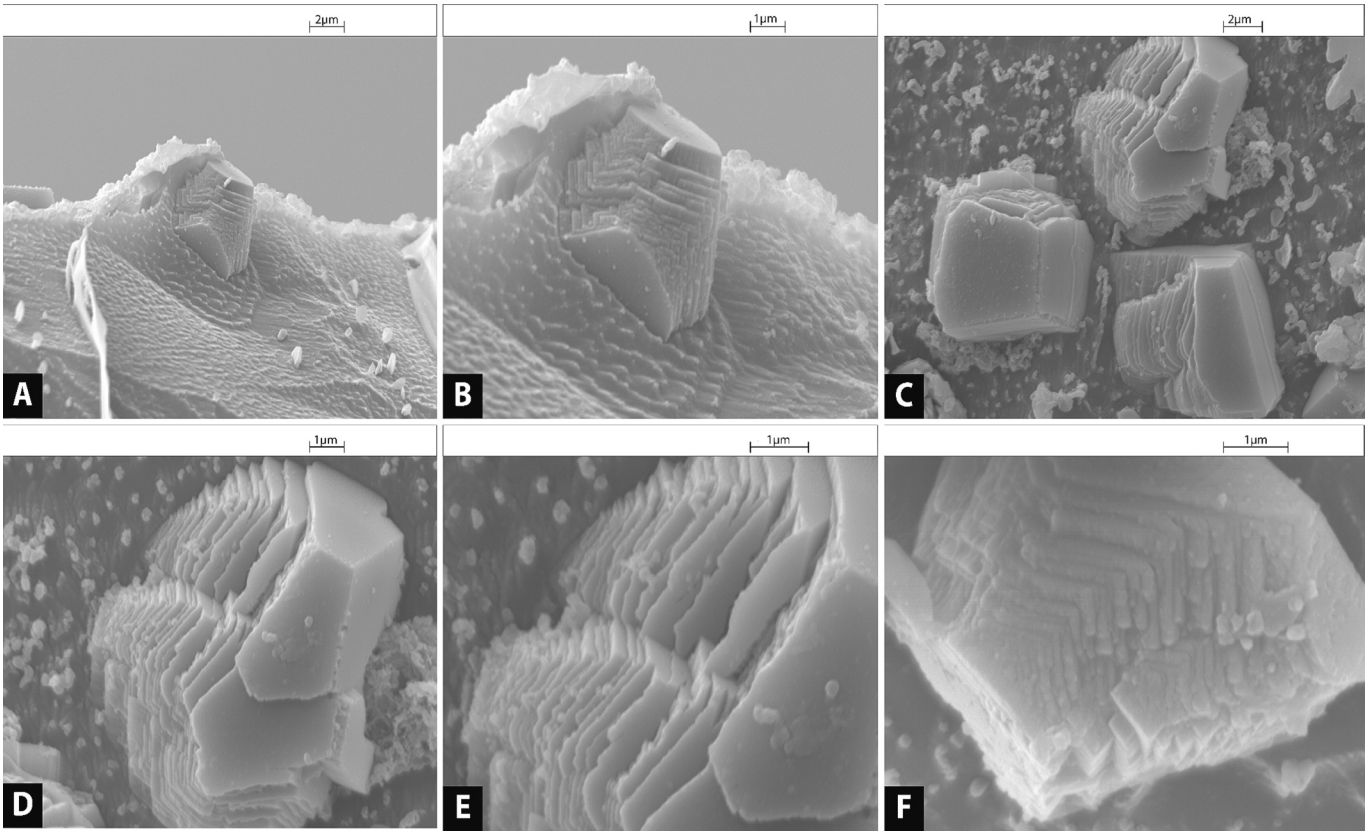


**Fig. 8.** SEM images of the Consett freshwater sample C1.

**Table 3**
Depicting the different partition coefficients for the elements seqauestered in the sample of ikaite versus the partition coefficients of calcite and aragonite from the literature.

| Measured values | | Literature data | | | |
|---|---|---|---|---|---|
| Metal | Partition coefficient (ikaite) | Partition coefficient range (calcite) | Reference | Partition coefficient range (aragonite) | Reference |
| Ba | 130.38 | 0.04–1.2 | Pingitore and Eastman (1984)<br>Olsson et al. (2014) | 1.48 | Kretz (1982) |
| Cu | 3331.97 | 23.3–50 | Kitano et al. (1980)<br>Olsson et al. (2014) | | |
| Cd | 116.26 | 4.5–66.1 | Lorens (1981)<br>Olsson et al. (2014) | | |
| Pb | 3761.41 | 0.64 | Morse and Luther Iii (1999) | | |
| Sr | 196,598.92 | 0.15–0.40 | Mucci and Morse (1983) | 0.22–1.83 | Kitano et al. (1980) Kretz (1982) |
| V | 30.44 | | | | |
| Cr | 62.82 | 0.10 | Kitano et al. (1980) | | |
| Mn | 419.15 | 3.1–13.1 | Dromgoole and Walter (1990)Olsson et al. (2014) | | |
| Ni | 41.57 | 0.15–1 | Lakshtanov and Stipp (2007)<br>Olsson et al. (2014) | | |
| Zn | 175.80 | 0.90–27 | Kitano et al. (1980)<br>Olsson et al. (2014) | | |

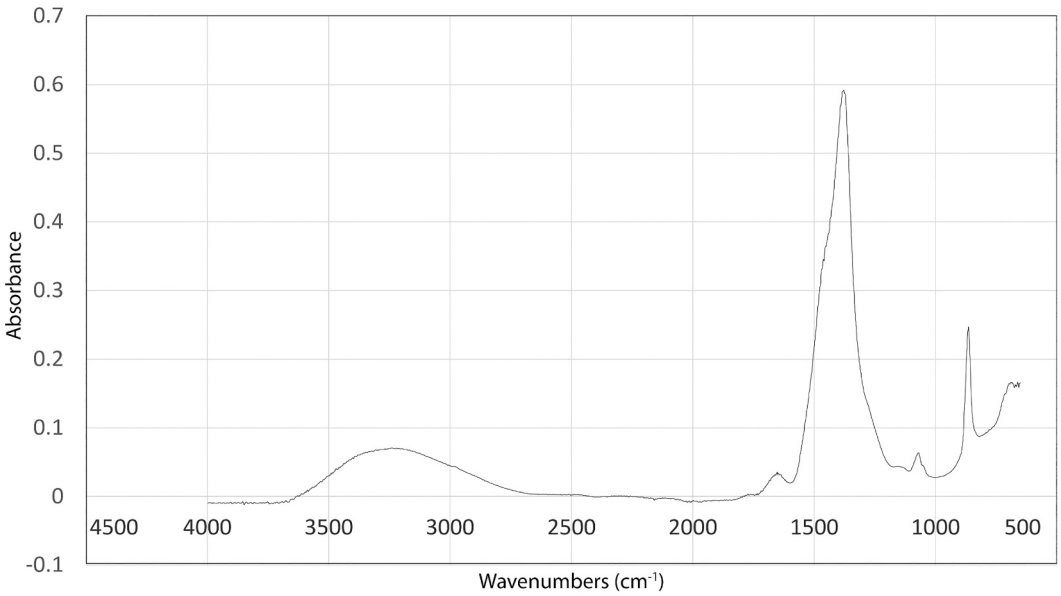


**Fig. 9.** Trial of making ikaite following the method of Lennie et al. (2004) corresponding to ACC.

symmetric vibration at 725 $cm^{-1}$, which is diagnostic of crystalline calcium carbonate phases only (Rodriguez-Blanco et al., 2011). The non-crystalline nature of these samples was confirmed by XRD, which showed no x-ray scattering and thus very poor crystallinity. Therefore, the laboratory experiments have not allowed to synthesize ikaite.

## 4. Discussion

### 4.1. Discovery of ikaite in steel waste leachate

We present the first report of ikaite formed in steel slag leachate sites where these transient growths may alter the dynamics of environmentally harmful elements. The sample we describe was recovered during a period with average air temperature of 1.1 °C and water temperature of 9.9 °C, and the previous two nights had minimum average temperature of −4.1 °C (CEDA Archive from the nearest station, Durham).

This is within the stability range for ikaite (<−4–8 °C) defined by Boch et al. (2015). Similar transient development of ikaite in steel-waste affected surface water may be very widespread, especially in the northern hemisphere. This potential is illustrated in Fig. 11, which shows a range of major steel-producing sites at high and mid latitudes which are candidates for this process spanning Canada (Nova Scotia), Great Lakes of the USA, Sweden, Finland, UK, France, Germany, Romania, Russia (Siberia), Ukraine, Kazakhstan, China and Japan. Of particular concern are sites in Russia, Canada, and USA, where the winters are cold enough for ikaite precipitates to accumulate for many months. Indeed, winters are likely to be cold enough to facilitate ikaite precipitation for 5 months at sites in Russia, 3 months in Canada, 3 months in the USA.

The ikaite crystals seen in the field (Fig. 3) are not embedded within the permanently sedimented calcite. Indeed, the cm-sized euhedral to subhedral white crystals are dominantly located along the barrage crests

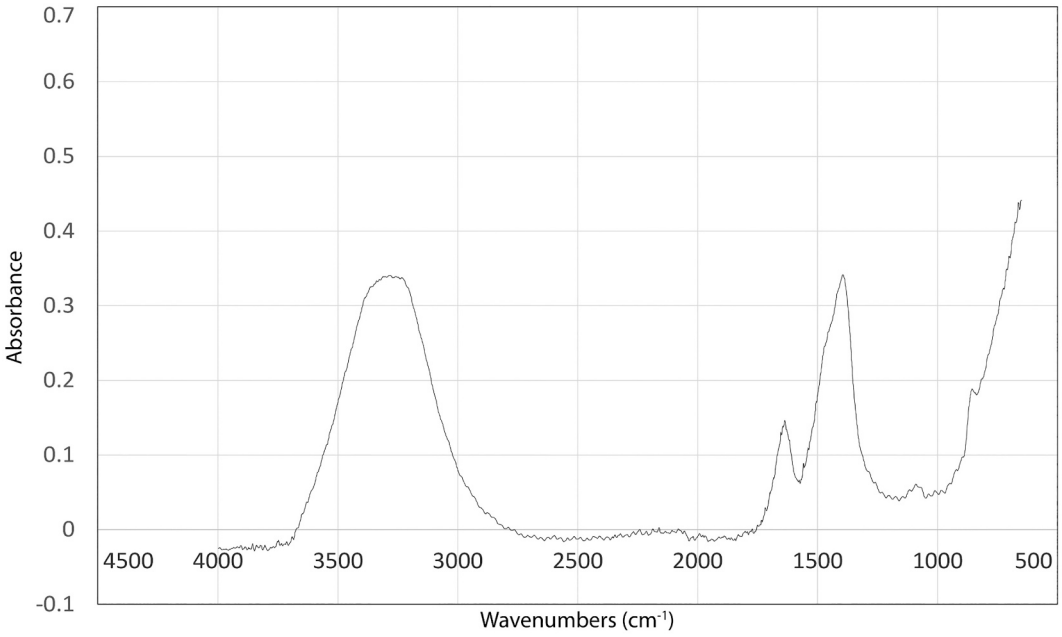


**Fig. 10.** Trial of making ikaite following the method of Tollefsen et al. (2020) corresponding to ACC.

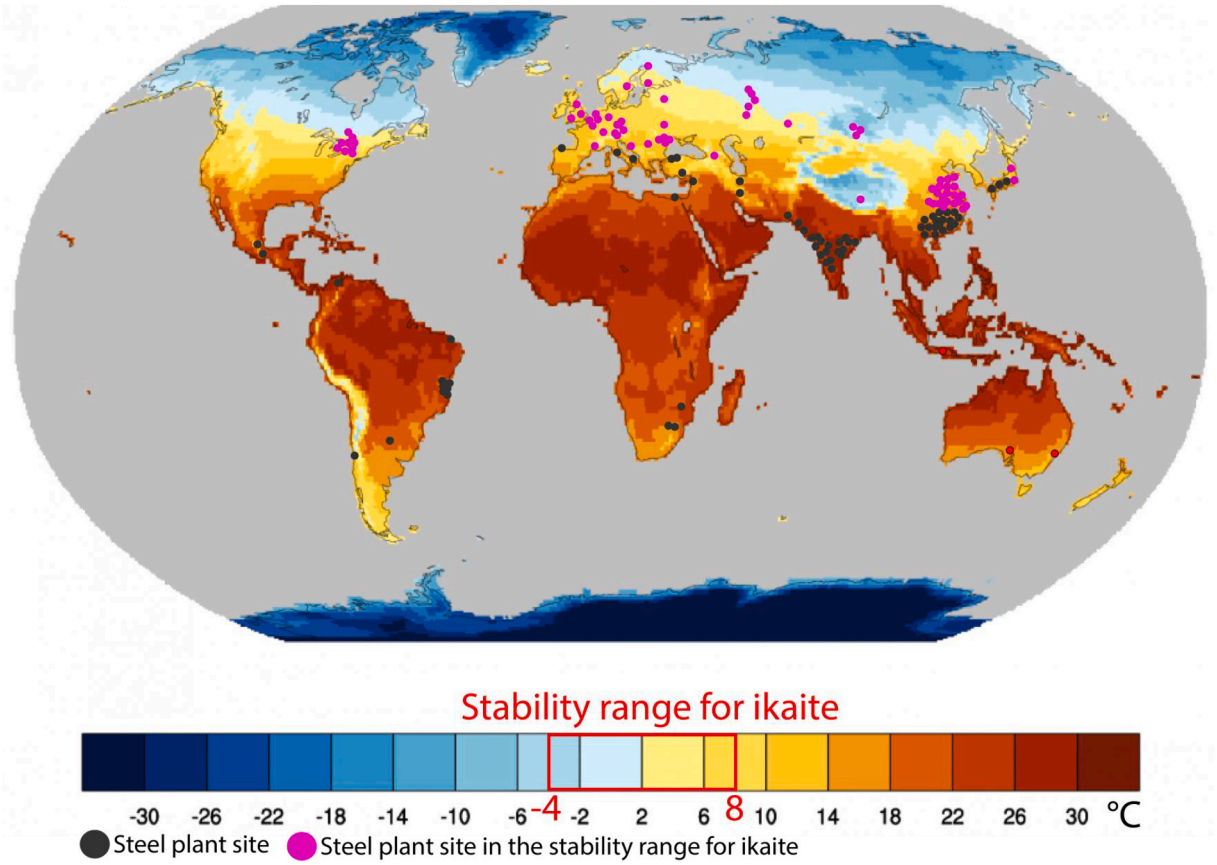


**Fig. 11.** Climatology of annual mean land temperature for 1951–1980 from the Berkeley Earth data after NCAR, ClimateDataGuide with the overlapped localization of the countries with annual mean land temperature lower than 8 °C and steel plant sites after World steel plant maps - 2020 Geography (https://www.steelonthenet.com/maps.html).

(Fig. 3), are thus forming at the water-air interface where low air temperatures will most strongly affect the solution. The sampled carbonate precipitate of white crystalline material exhibits a grainy consistency (Fig. 3), and although we do find minor calcite within the XRD data we have not found ikaite-shaped cavities, or replacement textures like thinolite or glendonite within these deposits. Therefore, the ikaite must disintegrate, returning its content to solution. Ikaite is more susceptible to re-dissolution and mechanical abrasion compared to calcite due to a

combination of chemical and mechanical processes. Consequently, ikaite is subject to vanish rapidly from the barrage crests, i.e. probably within a few days when the cold weather ceases (Boch et al., 2015).

This transient mineral formation is a new type of potential significant but inherently unstable contaminant sink for these sites, confirming the hypothesis of Boch et al. (2015). In the sample reported here, the partition coefficients are higher than 1 for all investigated contaminants with the exception of vanadium (Table 3), which is more likely to sink to Fe-oxide phases in alkaline systems (Hobson et al., 2018). In sites where ikaite develops only briefly and is unable to generate large inventories of contaminants, this represents only a modest complication for contaminant pathways. However, given that cold periods favourable to ikaite accumulation may occur for 3–5 months of the year in the world's most northerly steel manufacturing sites, the impact of this process is likely to be much more severe and environmentally detrimental in these areas (Boch et al., 2015). Indeed, the duration of storage of ikaite is controlled by the duration of the cold period (i.e., climate). This duration corresponds to days in County Durham but would be weeks or months in a colder climate location. The size of the issue would be therefore amplified by the duration of the ice-forming period in the winter months. Accumulation during cold winter periods followed by rapid increase in springtime temperature will likely result in a "saw tooth" pattern in pollutant dynamics, unlike the behaviour of more permanent inventories (Boch et al., 2015). Although there could be the moderating influence of dilution capacity offered by snowmelt-controlled hydrographs in high latitude areas, monitoring any pollutant release would be logistically challenging. Any release event would also likely evade ambient downstream monitoring given this is typically undertaken fewer than 5 times per year (EA Water Quality Archive, 2022, for Ebchester station: NE-43400174). That is not to say that these contamination pulses are environmentally negligible, particularly closer to the source sites, and their composition and impact are discussed in further detail below.

It remains possible that conversion of ikaite to microcrystalline calcite allows some stable carbonate precipitates to remain in the riverbed, reducing the severity of the rapid mass release during warming. This is known to occur from other places of original ikaite formation (Omelon et al., 2001; Oehlerich et al., 2013). After thermal decomposition, the solid crusts are easily stripped-off and mobilized in the turbulent water flow (Boch et al., 2015). This detrital calcite would represent a more permanent sink than ikaite but will further complicate dynamics at these sites and will require further field and experimental investigation.

### 4.2. What contaminant phases are likely to be accumulated into a transient ikaite inventory?

Where the ikaite inventory preferentially accumulates an environmental contaminant (i.e. the contaminant has a partition coefficient higher than 1), this will amplify the saw-tooth dynamics by enriching the transient reservoir. In the sample reported here, the partition coefficients are higher than 1 for all investigated contaminants with the exception of vanadium (Table 3). Rapid release during warming of an inventory so strongly enriched in a range of contaminants compared to the ambient water would pose a very severe challenge to aquatic and riparian ecosystems and may extend far downstream of the area exhibiting ikaite growth. These release events would likely evade standard monitoring approaches, which generally focus on sampling at regular, widely spaced intervals. The process of formation-dissolution of ikaite is faster than the spacing between those samplings in our UK site. The average sampling spacing in recent years (February 2018 until October 2019) is quite infrequent (0.38 per month: 4–5 times in one year) at the nearest site from our UK site, downstream of Consett Sewage Treatment works at Ebchester (Sampling point ID: NE-43400174), within Northumberland Durham and Tees after public sector information licensed under the Open Government Licence v3.0. Since the location of this site (downstream of Consett Sewage Treatment works), it does constitute the closest semi-active station to our UK site, enabling to record a flushing event. At colder sites where winter ikaite inventories are higher, the release event may still be over within a few days during the spring thaw be similarly irresolvable.

Monitoring of bulk solution properties such as pH to identify ikaite disintegration releases may also be challenging, as the carbonate release to solution will be masked by already high $CO_3^{2-}$ and $OH^-$ alkalinity. Conductivity monitoring is the most likely bulk parameter to resolve these changes, but as the ratio of contaminant: Ca would be higher during the release event, such measurements would still significantly under-estimate the impact. We find that if ikaite is identified within similar systems to that described here, monitoring procedures will need to be redesigned to capture acute contamination periods during ikaite disintegration.

### 4.3. Why are these elements enriched in ikaite compared to the solution?

The partition coefficients reported here are significantly higher than those reported in the literature for other calcium carbonate polymorphs, and some (e.g. Sr, which is enriched in the mineral by over 1000,000 times compared to solution) are very high indeed. It seems likely that were sufficient Sr available in solution, a hydrated strontium carbonate polymorph would have been formed. Although as far as we are aware these are the first partition coefficients of our ikaite field sample provided in the literature, these extreme behaviours demand further investigation.

#### 4.3.1. Laboratory synthesis experiments

Using two different published methodologies for ikaite synthesis, we found the initial precipitate was actually ACC, as determined by FTIR measurements (Figs. 9 and 10). Ikaite was formed as a secondary phase if the precipitate was stored under cool conditions ($-4.35 - +1.1$ °C for at least 7 days). We note 3 months storage is recommended as part of the synthesis for ikaite in the protocol published by Lennie et al. (2004). We also note that Tollefsen et al. (2020) report that ikaite precipitated in their experiments together with ACC at temperatures between 10 °C and 35 °C, and the amount of ACC increased with temperature. At 35 °C, the sample contained 94% ACC. Such formation of ikaite from precursor ACC has previously been reported (Chaka, 2018), and seems a generalisable feature of formation of this mineral in conditions analogous to nature. The electron microscope images of our field sample (Fig. 8) show ikaite crystals growing, but no clear evidence for ACC. However, replacement may be very rapid and could have completed before our time of sampling, so it remains possible that there was indeed an amorphous pre-cursor at this site.

Initial precipitation as an ACC phase may explain why partition coefficients we report from Consett are very high, as the disordered structure of amorphous mineral permits easy incorporation of trace elements. In an analogous series of experiments, conversion of ACC to calcite by dissolution-reprecipitation result in final mineral composition with enhanced partition coefficients for Li, Sr, Mg, U, B, Ba, and elements multiplied respectively by up to 3, 4, 8, 16, 565 and 1500 times respectively, (See Table 2 of Ulrich et al., 2021). Since an ordered mineral is not actually being produced direct from solution in these systems, the thermodynamics of aqueous crystal assembly is not relevant to final crystal composition. Rather, composition is set by the sequential partitioning of the water to ACC reaction, and the ACC to ikaite reaction. One potential benefit of this behaviour is that there is potential for very high toxic trace element content to be transferred another Ostwald step forward if ikaite does dehydrate to calcite during warming, permanently sequestering the pollutants. The Ostwald's step rule states that on the law of successive reactions, it is not the stablest state with the least amount of free energy that is initially obtained, but the least stable one, lying nearest to the original state in free energy (Van Santen, 1984). Further research is needed to determine the balance of harmful elements

and barium sequestered to the ikaite inventory, which is ultimately transferred to the calcite inventory, or returned to solution.

### 4.4. What is the environmental risk posed by this finding?

Mayes et al. (2018) established a maximum rate of carbonate production per day in Howden Burn of 259 g.m.$^{-2}$ day$^{-1}$. Assuming that under cold conditions as experienced during the fieldwork reported, all of this mass is deposited as ikaite it is possible to use the partition behaviour described above to estimate how much of each contaminant would be stored in ikaite during the cold spell in early 2019. These are shown in Table 4. Cadmium, chromium and nickel are likely to be sequestered at a rate close to 16–230 mg m$^{-2}$ day$^{-1}$, zinc and barium in a range of 680–2400 mg m$^{-2}$ day$^{-1}$ and manganese and lead at exceptionally high rates of 5800 and 22,000 mg m$^{-2}$ day$^{-1}$ respectively (See Table 4). If accumulation continued throughout the approximately week-long cold spell, estimates for the amount of lead stored in the transient ikaite inventory may approach 200 g m$^{-2}$ so long as sufficient Pb was available in the solution. This entire inventory may be released back to solution in a matter of hours during warming.

It is interesting to note that the absolute concentrations in ikaite are consistently above published values for the bulk carbonate crusts in the terraces (Table 5). The concentrations in ikaite are 10 times higher in order of magnitude for Ba, Mn and Zn, 100 times higher for Cd, Cr, Ni and 1000 times higher for Pb.

For specific spatial regions such as Russia, North of America, Canada, Sweden, Finland, Central Europe, where winter can provide conditions at least as cold as Consett for several months, this issue may become acute. Large masses of toxic trace elements accumulated in ikaite and the released in a short duration would cause acute pollution events during thaw periods. We recommend that this impact is investigated, as it may cause river health to be considerably lower than standard monitoring practices would explain. Complicating this further, Tollefsen et al. (2020) demonstrate ikaite forming under ambient temperatures of a much higher range than generally given, extending as high as 35 °C. Consequently, it remains possible that minor ikaite formation in steel waste affected sites may be very widespread indeed.

Alternatively, ikaite often undergoes solid state dehydration, which may not release metals in this manner. Under this mechanism, the formation of ikaite would be providing an environmentally useful additional sequestration of these harmful metals and metalloids. Regardless, further work needs to 1) determine whether solid state dehydration is happening in this context, 2) that this happens conservatively, providing enhanced sequestration of toxic metals and metalloids during the winter and 3) if this is not occurring, how severe the harmful contaminant pulses are.

### 4.5. How harmful would release of these contaminants in a transient mineral inventory likely be?

Specific concern arises from this investigation for springtime peaks in contamination with chromium, manganese, nickel, zinc, cadmium, barium, and lead (Table 3). There is less preoccupation regarding strontium and copper as for Sr, our system does not infer any radioactivity and for Cu, concentrations are low and usually either around limits of detection (LOD) or if not, there are below aquatic life standards. All aside from manganese and barium are heavy metals which have a marked effect on the aquatic flora and fauna. These toxic metals entering in aquatic environment are adsorbed onto particulate matter, although they can form free metal ions and soluble complexes that are available for uptake by biological organisms (Lokhande et al., 2011), and through bio-magnification can enter the food chain, ultimately affecting human populations as well (Lokhande et al., 2011). The toxic effects of heavy metals such as chromium, cadmium, zinc, and lead can affect the individual growth rates, physiological functions, mortality and reproduction in fish (Ali et al., 2014). Heavy metals entre in fish bodies by three possible ways: by gills, by digestive track and body surface (Lokhande et al., 2011). The gills are considered as the significant site for direct uptake of metals from the water, though the body surface is normally estimated to take minor part in uptake of heavy metals in fish (Abdul-Wahab and Marikar, 2012).

As reviewed by Ali et al. (2014), heavy metal accumulation, such as Cr and Cd, in fish severely affects their health and are of primary ecological importance (Table 6). When passed into the human food supply, fish contaminated with Pb, Cr, Cd and Zn cause great concern for human health (Juberg et al., 1997; Rossi and Jamet, 2008; Healey, 2009). These contaminants constitute priority hazardous substances affecting human health and aquatic life (Table 6). The impact of Ba, Mn and Ni is rather different to the heavy metals described above but can be severe for plant and animal systems. These elements correspond to secondary hazardous substances and their toxicity is reported in Table 6.

**Table 4**
Depicting the rate of contaminants stored in ikaite per day for each metal.

| Metal | Rate of contaminants stored in ikaite per day (mg.m$^{-2}$.day$^{-1}$) |
|---|---|
| Ba | 2404.60 |
| Cr | 228.99 |
| Mn | 5820.35 |
| Ni | 160.57 |
| Zn | 686.58 |
| Cd | 16.20 |
| Pb | 22,122.46 |

**Table 5**
Concentrations of elements of interest in ikaite samples (this study; $n = 1$; median shown) against bulk analysis of carbonate terraces at the Howden Burn site (data from Mayes et al., 2008; median shown with range in parenthesis: $n = 3$).

| Metal | Concentration of ikaite sample (ppm) | Concentration of carbonate terraces (ppm) |
|---|---|---|
| Ba | 672.7 | 70 (31–140) |
| Cd | 11.2 | 0.5 (0.4–0.5) |
| Cr | 124.8 | 6.4 (3.0–15.3) |
| Mn | 1389.9 | 200 (190–240) |
| Ni | 106.1 | 1.7 (1.4–1.7) |
| Pb | 15,975.1 | 20.1 (14.4–30.2) |
| Zn | 398.9 | 20 (17–38) |

## 5. Conclusion

Ikaite formation presented in this study occurs in an anthropogenic system within steel-slag leachate and is the first documentation worldwide for this setting of ikaite crystallization. This was achieved through a novel combination of in-situ FTIR analysis to inform sample selection for XRD analysis, which could provide a model for identifying ikaite at similar sites in the temperate zone. We deduce from laboratory experiments and very high partition coefficients in the field sample that ikaite is a secondary mineral with a primary phase being ACC. The ikaite forming in steel-slag leachate affected waters is incorporating large inventories of very harmful pollutants such as the heavy metals cadmium and lead which are most toxic to all human beings, animals, fishes, and environment. Chromium, zinc, manganese, barium and nickel are other potent contaminants reported in this study that preferentially accumulate in the transient ikaite inventory. Masses accumulated in ikaite may be very high, with g.m$^{-2}$.day$^{-1}$ estimated for lead.

As ikaite is thermally unstable, the inventory is lost during warming periods. In our field study area (Consett, County Durham, UK) this is related to synoptic weather, but in colder regions the warming will likely relate to springtime thawing. It is unclear how much ikaite is converted to calcite by dehydration, but at Consett we find no direct evidence of this. Consequently, most of the temporarily stored contaminant mass will be lost back to solution in a short duration, creating a significant peak in toxicity. These short-lived periods of acute pollution may have

**Table 6**
Depicting the potential impacts of the different contaminants classified by primary ecological importance, priority, and secondary hazardous substances.

| PRIMARY ECOLOGICAL IMPORTANCE (Affecting health of fish) | |
|---|---|
| Element | **Potential impacts** |
| Cd | Cadmium can reduce the reproduction rate of aquatic organisms, and continual exposure to cadmium can lead to a gradual extinction of affected taxa (Ali et al., 2014). Cadmium damages the kidney and produces signs of chronic toxicity, including impaired reproductive capacity and kidney function, tumors, hypertension and hepatic dysfunction. Sub-lethal concentrations of Cadmium cause deviations on the electrophoretic arrangements of protein segments in gills and muscle O.mossambicus (ibid) (Ali et al., 2014). |
| Zn | Zinc is a potential toxicant to fish (Vosylienė and Mikalajūnė, 2006) which causes disturbances of acid-base and ion regulation, disruption of gill tissue and hypoxia ( Murugan et al., 2008). The underlying cause of these impacts is zinc accumulating in the gills and reducing tissue respiration leading to tohypoxia, which results in death. Zinc pollution also promotes changes in ventilator and heart physiology (Olaifa et al., 1998). Sub-lethal levels of zinc have been known to unfavorably affect hatchability, existence and hematological strictures of fish (Olaifa et al., 1998), deficiency of balance since most fins are stationary in the affected fish, restless swimming, air guzzling, periods of dormancy and death (Kori-Siakpere and Ubogu, 2008). |

| PRIORITY HAZARDOUS SUBSTANCES (Affecting human health and aquatic life) | |
|---|---|
| Element | Potential impacts |
| Pb | Lead is a recognised and potent environmental pollutant, which accumulates in muscles, bones, blood and fat (Ali et al., 2014). This results in severe damage to liver, kidneys, brain, nerves and other organs, especially in young individuals and infants. Exposure to lead may also lead to reproductive disorders osteoporosis (brittle bone disease), causes increases in heart disease, high blood pressure, and affects the blood and heart causes anemia and affects the nerves and brain (Ali et al., 2014). Extensive exposure to lead causes memory problems appropriations, behavioral disorders, mental retardation while lesser levels of lead damage the nerves and brain in fetuses and young children, resulting in lowered IQ and learning deficits (ibid). |
| Cr | Chromium toxicity in humans can cause faded immune system, skin diseases, ulcers and digestive problems, alteration in genetic material, liver and kidney damage, death ( Karadede et al., 2004). |
| Cd | Cadmium can damage the kidneys, causing the excretion of sugars and essential proteins from the body and cause diarrhoea, vomiting, stomach problems, fractures in bone, damage to DNA, failure in reproduction and fertility, cause damage to nervous system, damage to immune system and some cancers (Abdul-Wahab and Marikar, 2012). Elevated levels of zinc can cause skin annoyances, stomach cramps, anemia, vomiting and nausea (Lokhande et al., 2011). |
| Zn | High levels of Zn damages the pancreas and disturb the protein metabolism, and cause arteriosclerosis (Abdul-Wahab and Marikar, 2012). |

| SECONDARY HAZARDOUS SUBSTANCES (Affecting plant and animal systems) | |
|---|---|
| Element | **Potential impacts** |
| Ba | It has been shown to reduce photosynthesis, chlorophyll fluorescence and stomatal resistance in plants (Abdul-Wahab and Marikar, 2012). This results in reduced biomass production in beans (Chaudhry et al., 1977; Llugany et al., 2000) and soybeans (Suwa et al., 2008) due to reduced $CO_2$ assimilation caused by limited photosynthetic activity (Melo et al., 2011). Barium has also been shown to affect a variety of cellular and developmental processes in both plant and animal systems (Spangenberg and Cherr, 1996). These include perturbation of vitellogenin uptake in insect follicles (Kindle et al., 1990), inhibition of ciliary function in trochophore larvae (Marsden and Hassessian, 1986), and structural and functional integrity of flagella in algae (Zmarzly and Lewin, 1986). It has been suggested that these effects result from Ba interaction with cellular Ca homeostasis (Spangenberg and Cherr, 1996). |
| Mn | Plants have been shown to react to excess Mn with a drop-in photosynthetic rate (Macfie and Taylor, 1992; Macfie et al., 1994). This lowering of photosynthesis occurred as a result of decreases in chlorophyll and the photosynthesis per unit chlorophyll in a sensitive cultivar and only reducing the chlorophyll content in a tolerant cultivar of *T. aestivum* (Moroni et al., 1991; Macfie and Taylor, 1992). Manganese toxicity has also been associated with swollen chloroplasts in *G.* max (Wu, 1994). |
| Ni | Excess Ni has been reported to cause leaf necrosis and chlorosis of plants (Chen et al., 2009). Chlorosis and along-vein necrosis appeared in newly developed leaves of water spinach after plants were treated with 0.085 to 0.255 mM (5–15 ppm) Ni for a week (Sun and Wu, 1998). Ni at a concentration of 0.5 mM produced dark brown necrotic spots along the leaf margins and decreased water potential and transpiration rate, resulting in wilting of outer leaves and necrosis of inner leaves of cabbage (Pandey and Sharma, 2002). Barley grown in 0.1 mM Ni for 14 days showed chlorosis and necrosis of leaves (Rahman et al., 2005). |

adverse effects on receiving waters. The regions most exposed to this risk as those with long durations of stable low temperature in the winter, so steel-making and former steel-making locations in Russia, northern North America, Canada, Sweden, Finland and Central Europe should be investigated for this process. Ikaite is considered to have an upper temperature limit of 8 °C, providing a key isotherm to guide this investigation spatially and seasonally. However, ikaite has been reported forming under ambient temperatures (5–35 °C), so the 8 °C isotherm may significantly underestimate the issue.

In summary, we have (1) documented the presence of the carbonate mineral ikaite as a secondary mineral percolating from high Ph industrial wastewaters during periods of cold weather, (2) demonstrated that ikaite can act as a significant sink for hazardous metalliferous contaminants and (3) revealed how the inherent thermal instability of ikaite may lead to impactful pulsed releases of higher concentrations of contaminants into the natural environment during the spring thaw at high latitudes.

Supplementary data to this article can be found online at https://doi.org/10.1016/j.chemgeo.2023.121842.

## Declaration of Competing Interest

The authors declare that they have no known competing financial interests or personal relationships that could have appeared to influence the work reported in this paper.

## Data availability

Data will be made available on request.

## References

Abdul-Wahab, S., Marikar, F., 2012. The environmental impact of gold mines: pollution by heavy metals. Open Eng. 2 (2), 304–313.
Ali, A.S., US, S. A, Ahmad, R., 2014. Effect of different heavy metal pollution on fish. Res. J. Chem. Env. Sci 2 (1), 74–79.
Barber, D.G., Ehn, J.K., Pućko, M., Rysgaard, S., Deming, J.W., Bowman, J.S., Søgaard, D. H., 2014. Frost flowers on young Arctic Sea ice: the climatic, chemical, and microbial significance of an emerging ice type. J. Geophys. Res. Atmos. 119 (20), 11–593.
Bastianini, L., Rogerson, M., Mercedes-Martín, R., Prior, T.J., Cesar, E.A., Mayes, W.M., 2019. What causes carbonates to form "shrubby" morphologies? An Anthropocene limestone case study. Front. Earth Sci. 7, 236.
Bastianini, L., Mayes, W., Rogerson, M., Prior, T., Mercedes Martín, R., 2021. What Are the Different Styles of Calcite Precipitation within a Hyperalkaline Leachate? A

Sedimentological Anthropocene Case Study. Depositional Record. https://doi.org/10.1002/dep2.168.
Besselink, R., Rodriguez-Blanco, J.D., Stawski, T.M., Benning, L.G., Tobler, D.J., 2017. How short-lived Ikaite affects calcite crystallization. Cryst. Growth Des. 17 (12), 6224–6230.
Bischoff, J.L., Stine, S., Rosenbauer, R.J., Fitzpatrick, J.A., Stafford Jr., T.W., 1993. Ikaite precipitation by mixing of shoreline springs and Lake water, Mono Lake, California, USA. Geochim. Cosmochim. Acta 57 (16), 3855–3865.
Boch, R., Dietzel, M., Reichl, P., Leis, A., Baldermann, A., Mittermayr, F., Pölt, P., 2015. Rapid ikaite (CaCO3· 6H2O) crystallization in a man-made river bed: hydrogeochemical monitoring of a rarely documented mineral formation. Appl. Geochem. 63, 366–379.
Brečević, L., Nielsen, A., 1993. Solubility of calcium carbonate hexahydrate. Acta Chem. Scand. 47, 668–673.
Brooks, R., Clark, L.M., Thurston, E.F., 1950. Calcium carbonate and its hydrates. Philosophical transactions of the royal society of London. Series A, Mathemat. Phys. Sci. 243 (861), 145–167.
Buchardt, B., Seaman, P., Stockmann, G., Vous, M., Wilken, U., Düwel, L., Petersen, G.H., 1997. Submarine columns of ikaite tufa. Nature 390 (6656), 129–130.
Carteret, C., Dandeu, A., Moussaoui, S., Muhr, H., Humbert, B., Plasari, E., 2009. Polymorphism studied by lattice phonon Raman spectroscopy and statistical mixture analysis method. Application to calcium carbonate polymorphs during batch crystallization. Cryst. Growth Des. 9 (2), 807–812.
Chaka, A.M., 2018. Ab initio thermodynamics of hydrated calcium carbonates and calcium analogues of magnesium carbonates: implications for carbonate crystallization pathways. ACS Earth and Space Chem. 2 (3), 210–224.
Chakrabarty, D., Mahapatra, S., 1999. Aragonite crystals with unconventional morphologies. J. Mater. Chem. 9 (11), 2953–2957.
Chaudhry, F.M., Wallace, A., Mueller, R.T., 1977. Barium toxicity in plants. Commun. Soil Sci. Plant Anal. 8 (9), 795–797.
Chen, C., Huang, D., Liu, J., 2009. Functions and toxicity of nickel in plants: recent advances and future prospects. Clean–soil, air, water 37 (4–5), 304–313.
Coleyshaw, E.E., Crump, G., Griffith, W.P., 2003. Vibrational spectra of the hydrated carbonate minerals ikaite, monohydrocalcite, lansfordite and nesquehonite. Spectrochim. Acta A Mol. Biomol. Spectrosc. 59 (10), 2231–2239.
Cornelis, G., Johnson, C.A., Van Gerven, T., Vandecasteele, C., 2008. Leaching mechanisms of oxyanionic metalloid and metal species in alkaline solid wastes: A review. Appl. Geochem. 23 (5), 955–976.
Demichelis, R., Raiteri, P., Gale, J.D., Quigley, D., Gebauer, D., 2011. Stable prenucleation mineral clusters are liquid-like ionic polymers. Nat. Commun. 2 (1), 1–8.
Demichelis, R., Raiteri, P., Gale, J.D., 2014. Structure of hydrated calcium carbonates: A first-principles study. J. Cryst. Growth 401, 33–37.
Dempster, T., Jess, S.A., 2015. Ikaite pseudomorphs in Neoproterozoic Dalradian slates record Earth's coldest metamorphism. J. Geol. Soc. Lond. 172 (4), 459–464.
Dieckmann, G.S., Nehrke, G., Papadimitriou, S., Göttlicher, J., Steininger, R., Kennedy, H., Thomas, D.N., 2008. Calcium carbonate as ikaite crystals in Antarctic Sea ice. Geophys. Res. Lett. 35 (8).
Dromgoole, E.L., Walter, L.M., 1990. Iron and manganese incorporation into calcite: Effects of growth kinetics, temperature and solution chemistry. Chem. Geol. 81 (4), 311–336.
Field, L.P., Milodowski, A.E., Shaw, R.P., Stevens, L.A., Hall, M.R., Kilpatrick, A., Ellis, M. A., 2017. Unusual morphologies and the occurrence of pseudomorphs after ikaite (CaCO3· 6H2O) in fast growing, hyperalkaline speleothems. Mineral. Mag. 81 (3), 565–589.
Gandin, A., Capezzuoli, E., 2014. Travertine: distinctive depositional fabrics of carbonates from thermal spring systems. Sedimentology 61 (1), 264–290.
Gauldie, R.W., Sharma, S.K., Volk, E., 1997. Micro-Raman spectral study of vaterite and aragonite otoliths of the coho salmon, Oncorhynchus kisutch. Comp. biochem. physiol., Mol. 118 (3), 753–757.
Gebauer, D., Völkel, A., Cölfen, H., 2008. Stable prenucleation calcium carbonate clusters. Science 322 (5909), 1819–1822.
Glaring, M.A., Vester, J.K., Lylloff, J.E., Al-Soud, W.A., Sørensen, S.J., Stougaard, P., 2015. Microbial diversity in a permanently cold and alkaline environment in Greenland. PLoS One 10 (4).
Gomes, H.I., Mayes, W.M., Baxter, H.A., Jarvis, A.P., Burke, I.T., Stewart, D.I., Rogerson, M., 2018. Options for managing alkaline steel slag leachate: A life cycle assessment. J. Clean. Prod. 202, 401–412.
Greinert, J., Derkachev, A., 2004. Glendonites and methane derived Mg-calcites in the Sea of Okhotsk, Eastern Siberia: implications of a venting-related ikaite/glendonite formation. Mar. Geol. 204, 129–144.
Gunasekaran, S., Anbalagan, G., Pandi, S., 2006. Raman and infrared spectra of carbonates of calcite structure. J. Raman Spectros.: Int. J. Orig. Work Aspects Raman Spectros., Includ. Higher Order Process., Brillouin Rayleigh Scatter. 37 (9), 892–899.
Harber, A.J., Forth, R.A., 2001. The contamination of former iron and steel works sites. Environ. Geol. 40 (3), 324–330.
Harner, P.L., Gilmore, M.S., 2015. Visible–near infrared spectra of hydrous carbonates, with implications for the detection of carbonates in hyperspectral data of Mars. Icarus 250, 204–214.
Healey, N., 2009. Lead toxicity, vulnerable subpopulations and emergency preparedness. Radiat. Prot. Dosim. 134 (3–4), 143–151.
Hiruta, A., Matsumoto, R., 2022. Geochemical comparison of ikaite and methane – derived authigenic carbonates recovered from Echigo Bank in the Sea of Japan. Mar. Geol. 443, 106672.
Hobson, A.J., Stewart, D.I., Bray, A.W., Mortimer, R.J., Mayes, W.M., Riley, A.L., Rogerson, M., Burke, I.T., 2018. Behaviour and fate of vanadium during the aerobic neutralisation of hyperalkaline slag leachate. Sci. Total Environ. 643, 1191–1199.
Hu, Y.B., Wolf-Gladrow, D.A., Dieckmann, G.S., Völker, C., Nehrke, G., 2014. A laboratory study of ikaite (CaCO3· 6H2O) precipitation as a function of pH, salinity, temperature and phosphate concentration. Mar. Chem. 162, 10–18.
Hu, Y.B., Wolthers, M., Wolf-Gladrow, D.A., Nehrke, G., 2015. Effect of pH and phosphate on calcium carbonate polymorphs precipitated at near-freezing temperature. Cryst. Growth Des. 15 (4), 1596–1601.
Hull, S.L., Oty, U.V., Mayes, W.M., 2014. Rapid recovery of benthic invertebrates downstream of hyperalkaline steel slag discharges. Hydrobiologia 736 (1), 83–97.
Ito, T., 1996. Ikaite from cold spring water at Shiowakka, Hokkaido, Japan. J. Mm. Petr. Econ. Geol. 91, 209–219.
Ito, T., 1998. Factors controlling the transformation of natural ikaite from Shiowakka, Japan. Geochem. J. 32 (4), 267–273.
Jalilehvand, F., Spångberg, D., Lindqvist-Reis, P., Hermansson, K., Persson, I., Sandström, M., 2001. Hydration of the calcium ion. An EXAFS, large-angle X-ray scattering, and molecular dynamics simulation study. J. Am. Chem. Soc. 123 (3), 431–441.
Jansen, J.H.F., Woensdregt, C.F., Kooistra, M.J., Van der Gaast, S.J., 1987. Ikaite pseudomorphs in the Zaire deep-sea fan: an intermediate between calcite and porous calcite. Geology 15 (3), 245–248.
Juberg, D.R., Kleiman, C.F., Kwon, S.C., 1997. Position paper of the American Council on Science and Health: lead and human health. Ecotoxicol. Environ. Saf. 38 (3), 162–180.
Karadede, H., Oymak, S.A., Ünlü, E., 2004. Heavy metals in mullet, Liza abu, and catfish, Silurus triostegus, from the Atatürk Dam Lake (Euphrates), Turkey. Environ. Int. 30 (2), 183–188.
Kindle, H., Lanzrein, B., Kunkel, J.G., 1990. The effect of ions, ion channel blockers, and ionophores on uptake of vitellogenin into cockroach follicles. Dev. Biol. 142 (2), 386–391.
Kitano, Y., Okumura, M., Idogaki, M., 1980. Abnormal behaviors of copper (II) and zinc ions in parent solution at the early stage of calcite formation. Geochem. J. 14 (4), 167–175.
Kontoyannis, C.G., Vagenas, N.V., 2000. Calcium carbonate phase analysis using XRD and FT-Raman spectroscopy. Analyst 125 (2), 251–255.
Kori-Siakpere, O., Ubogu, E.O., 2008. Sublethal haematological effects of zinc on the freshwater fish, Heteroclarias sp.(Osteichthyes: Clariidae). Afr. J. Biotechnol. 7 (12).
Kristiansen, J., Kristiansen, A., 1999. A new species of Chroomonas (Cryptophyceae) living inside the submarine ikaite columns in the Ikkafjord, Southwest Greenland, with remarks on its ultrastructure and ecology. Nord. J. Bot. 19 (6), 747–758.
Lakshtanov, L.Z., Stipp, S.L.S., 2007. Experimental study of nickel (II) interaction with calcite: Adsorption and coprecipitation. Geochim. Cosmochim. Acta. 71 (15), 3686–3697.
Larsen, D., 1994. Origin and paleoenvironmental significance of calcite pseudomorphs after ikaite in the Oligocene Creede Formation, Colorado. J. Sediment. Res. 64 (3a), 593–603.
Lennie, A.R., Tang, C.C., Thompson, S.P., 2004. The structure and thermal expansion behaviour of ikaite, CaCO 3, 6H 2 O, from T= 114 to T= 293 K Mineral. Mag. 68 (1), 135–146.
Llugany, M., Poschenrieder, C., Barceló, J., 2000. Assessment of barium toxicity in bush beans. Arch. Environ. Contam. Toxicol. 39 (4), 440–444.
Lokhande, R.S., Singare, P.U., Pimple, D.S., 2011. Pollution in water of Kasardi River flowing along Taloja industrial area of Mumbai, India. World Environ. 1 (1), 6–13.
Longerich, H.P., Günther, D., Jackson, S.E., 1996. Elemental fractionation in laser ablation inductively coupled plasma mass spectrometry. Fresenius J. Anal. Chem. 355, 538–542.
Lorens, R.B., 1981. Sr, Cd, Mn and Co distribution coefficients in calcite as a function of calcite precipitation rate. Geochim. Cosmochim. Acta 45 (4), 553–561.
Lu, Z., Rickaby, R.E., Kennedy, H., Kennedy, P., Pancost, R.D., Shaw, S., Lennie, A., Wellner, J., Anderson, J.B., 2012. Anikaite record of late Holocene climate at the Antarctic Peninsula. EPSL 325, 108–115.
Macfie, S.M., Taylor, G.J., 1992. The effects of excess manganese on photosynthetic rate and concentration of chlorophyll in Triticum aestivum grown in solution culture. Physiol. Plant. 85 (3), 467–475.
Macfie, S.M., Cossins, E.A., Taylor, G.J., 1994. Effects of excess manganese on production of organic acids in Mn-tolerant and Mn-sensitive cultivars of Triticum aestivum L. (wheat). J. Plant Physiol. 143 (2), 135–144.
Marion, G.M., 2001. Carbonate mineral solubility at low temperatures in the Na-K-mg-ca-H-cl-SO4-OH-HCO3-CO3-CO2-H2O system. Geochim. Cosmochim. Acta 65 (12), 1883–1896.
Marland, G., 1975. The stability of CaCO3· 6H2O (ikaite). Geochim. Cosmochim. Acta 39 (1), 83–91.
Mayes, W.M., Younger, P.L., Aumônier, J., 2008. Hydrogeochemistry of alkaline steel slag leachates in the UK. Water Air Soil Pollut. 195 (1–4), 35–50.
Marsden, J.R., Hassessian, H., 1986. Effects of Ca2+ and catecholamines on swimming cilia of the trochophore larva of the polychaete Spirobranchus giganteus (Pallas).J. Exp. Mar. Biol. Ecol. 95 (3), 245–255.
Mayes, W.M., Jarvis, A.P., Burke, I.T., Walton, M., Feigl, V., Klebercz, O., Gruiz, K., 2011. Dispersal and attenuation of trace contaminants downstream of the Ajka bauxite residue (red mud) depository failure, Hungary. Environ. Sci. Technol. 45 (12), 5147–5155.
Mayes, W.M., Riley, A.L., Gomes, H.I., Brabham, P., Hamlyn, J., Pullin, H., Renforth, P., 2018. Atmospheric $CO_2$ sequestration in iron and steel slag: Consett, County Durham, United Kingdom. Environ. Sci. Technol. 52 (14), 7892–7900.

Melo, L.C.A., Alleoni, L.R.F., Carvalho, G., Azevedo, R.A., 2011. Cadmium-and barium-toxicity effects on growth and antioxidant capacity of soybean (Glycine max L.) plants, grown in two soil types with different physicochemical properties. J. Plant Nutr. Soil Sci. 174 (5), 847–859.
Mikkelsen, A., Andersen, A.B., Engelsen, S.B., Hansen, H.C.B., Larsen, O., Skibsted, L.H., 1999. Presence and dehydration of ikaite, calcium carbonate hexahydrate, in frozen shrimp shell. J. Agric. Food Chem. 47 (3), 911–917.
Milodowski, A.E., Shaw, R.P., Stewart, D.I., 2013. The Harpur Hill Site: Its Geology, Evolutionary History and a Catalogue of Materials Present. British Geological Survey, Keyworth, Nottingham, UK.
Montes-Hernandez, G., Renard, F., 2016. Time-resolved in situ raman spectroscopy of the nucleation and growth of siderite, magnesite, and calcite and their precursors. Cryst. Growth Des. 16 (12), 7218–7230.
Moroni, J.S., Briggs, K.G., Taylor, G.J., 1991. Chlorophyll content and leaf elongation rate in wheat seedlings as a measure of manganese tolerance. Plant Soil 136 (1), 1–9.
Morse, J.W., Luther Iii, G.W., 1999. Chemical influences on trace metal-sulfide interactions in anoxic sediments. Geochim. Cosmochim. Acta. 63 (19–20), 3373–3378.
Mucci, A., Morse, J.W., 1983. The incorporation of Mg2+ and Sr2+ into calcite overgrowths: influences of growth rate and solution composition. Geochim. Cosmochim. Acta. 47 (2), 217–233.
Murugan, S.S., Karuppasamy, R., Poongodim, K., Puvaneswari, S., 2008. Bioaccumulation Pattern of Zinc in Freshwater fish Channa punctatus (Bloch.) after Chronic Exposure. Turk. J. Fisher. Aqu. Sci. 8, 55–59.
Niedermayr, A., Köhler, S.J., Dietzel, M., 2013. Impacts of aqueous carbonate accumulation rate, magnesium and polyaspartic acid on calcium carbonate formation (6–40 C). Chem. Geol. 340, 105–120.
Oaki, Y., Imai, H., 2003. Experimental Demonstration for the Morphological Evolution of Crystals Grown in Gel Media. Cryst. Growth Des. 3 (5), 711–716.
Oehlerich, M., Mayr, C., Griesshaber, E., Lücke, A., Oeckler, O.M., Ohlendorf, C., Zolitschka, B., 2013. Ikaite precipitation in a lacustrine environment–implications for palaeoclimatic studies using carbonates from Laguna Potrok Aike (Patagonia, Argentina). Quat. Sci. Rev. 71, 46–53.
Ohlendorf, C., Fey, M., Massaferro, J., Haberzettl, T., Laprida, C., Lücke, A., Wille, M., 2014. Late Holocene hydrology inferred from lacustrine sediments of Laguna Cháltel (southeastern Argentina). Palaeogeogr. Palaeoclimatol. Palaeoecol. 411, 229–248.
Olaifa, F., Olaifa, A., Onwude, T., 1998. Lethal and sub-lethal effects of copper to the African catfish (Clariasgariepinus) Juveniles. Afr. J. Biomed. Res. 7, 45–53.
Olcott, A.N., Sessions, A.L., Corsetti, F.A., Kaufman, A.J., De Oliviera, T.F., 2005. Biomarker evidence for photosynthesis during Neoproterozoic glaciation. Science 310 (5747), 471–474.
Olsson, J., Stipp, S.L.S., Makovicky, E., Gislason, S.R., 2014. Metal scavenging by calcium carbonate at the Eyjafjallajökull volcano: A carbon capture and storage analogue. Chem. Geol. 384, 135–148.
Omelon, C.R., Pollard, W.H., Marion, G.M., 2001. Seasonal formation of ikaite (CaCO3·6H2O) in saline spring discharge at Expedition Fiord, Canadian High Arctic: Assessing conditional constraints for natural crystal growth. Geochim. Cosmochim. Acta 65 (9), 1429–1437.
Pandey, N., Sharma, C.P., 2002. Effect of heavy metals Co2+, Ni2+ and Cd2+ on growth and metabolism of cabbage. Plant Sci. 163 (4), 753–758.
Papadimitriou, S., Kennedy, H., Kennedy, P., Thomas, D.N., 2014. Kinetics of ikaite precipitation and dissolution in seawater-derived brines at sub-zero temperatures to 265 K. Geochim. Cosmochim. Acta 140, 199–211.
Pauly, H., 1963. "Ikaite", a new mineral from Greenland. Arctic 16 (4), 263–264.
Power, I.M., Wilson, S., Harrison, A.L., Dipple, G.M., McCutcheon, J., Southam, G., Kenward, P.A., 2014. A depositional model for hydromagnesite–magnesite playas near Atlin, British Columbia, Canada. Sedimentology 61 (6), 1701–1733.
Pingitore, N.E., Eastman, M.P., 1984. The experimental partitioning of Ba2+ into calcite. Chem. Geol. 45 (1–2), 113–120.
Power, I.M., Kenward, P.A., Dipple, G.M., Raudsepp, M., 2017. Room temperature magnesite precipitation. Cryst. Growth Des. 17 (11), 5652–5659.
Qu, Y., Teichert, B., Birgel, D., Goedert, J., Peckmann, J., 2017. The prominent role of bacterial sulfate reduction in the formation of glendonite: a case study from Paleogene marine strata of western Washington State. Facies 63, 10.
Rahman, H., Sabreen, S., Alam, S., Kawai, S., 2005. Effects of nickel on growth and composition of metal micronutrients in barley plants grown in nutrient solution. J. Plant Nutr. 28 (3), 393–404.
Riley, A.L., Mayes, W.M., 2015. Long-term evolution of highly alkaline steel slag drainage waters. Environ. Monit. Assess. 187 (7), 463.
Rodriguez-Blanco, J.D., Shaw, S., Benning, L.G., 2011. The kinetics and mechanisms of amorphous calcium carbonate (ACC) crystallization to calcite, via vaterite. Nanoscale 3 (1), 265–271.
Rogov, M., Ershova, V., Vereshchagin, O., Vasileva, K., Mikhailova, K., Krylov, A., 2021. Database of global glendonite and ikaite records throughout the Phanerozoic. Earth Syst. Sci. Data 13 (2), 343–356.
Rossi, N., Jamet, J.L., 2008. In situ heavy metals (copper, lead and cadmium) in different plankton compartments and suspended particulate matter in two coupled Mediterranean coastal ecosystems (Toulon Bay, France). Mar. Pollut. Bull. 56 (11), 1862–1870.
Rysgaard, S., Glud, R.N., Lennert, K., Cooper, M., Halden, N., Leakey, R.J.G., Barber, D., 2012. Ikaite crystals in melting sea ice-implications for pCO2 and pH levels in Arctic surface waters. Cryosphere 6 (4), 901.
Rysgaard, S., Søgaard, D.H., Cooper, M., Pućko, M., Lennert, K., Papakyriakou, T.N., McGinnis, D.F., 2013. Ikaite crystal distribution in winter sea ice and implications for CO2 system dynamics. Cryosphere 7, 707–718.
Shahar, A., Bassett, W.A., Mao, H.K., Chou, I.M., Mao, W., 2005. The stability and Raman spectra of ikaite, CaCO3· 6H2O, at high pressure and temperature. Am. Mineral. 90 (11−12), 1835–1839.
Shearman, D.J., McGugan, A., Stein, C., Smith, A.J., 1989. Ikaite, CaCO36H2O, precursor of the thinolites in the Quaternary tufas and tufa mounds of the Lahontan and Mono Lake Basins, western United States. Geol. Soc. Am. Bull. 101 (7), 913–917.
Sheldrick, G.M., 2015. Crystal structure refinement with SHELXL. Acta Crystallograph. Sec. C: Struct. Chem. 71 (1), 3–8.
Snyder, R.C., Doherty, M.F., 2007. Faceted crystal shape evolution during dissolution or growth. AICHE J. 53 (5), 1337–1348.
Spangenberg, J.V., Cherr, G.N., 1996. Developmental effects of barium exposure in a marine bivalve (Mytilus californianus). Environ. Toxicol. Chem.: Int. J. 15 (10), 1769–1774.
Stein, C.L., 1986. Authigenic carbonate nodules in the Nankai Trough, Site 583. Init. Repts. DSDP. 87, 659–668.
Stockmann, G., Tollefsen, E., Skelton, A., Brüchert, V., Balic-Zunic, T., Langhof, J., Karlsson, A., 2018. Control of a calcite inhibitor (phosphate) and temperature on ikaite precipitation in Ikka Fjord, Southwest Greenland. Appl. Geochem. 89, 11–22.
Stougaard, P., Jørgensen, F., Johnsen, M.G., Hansen, O.C., 2002. Microbial diversity in ikaite tufa columns: an alkaline, cold ecological niche in Greenland. Environ. Microbiol. 4 (8), 487–493.
Strohm, S.B., Inckemann, S.E., Gao, K., Schweikert, M., Lemloh, M.L., Schmahl, W.W., Jordan, G., 2022. On the nucleation of ikaite (CaCO3x6H2O)–A comparative study in the presence and absence of mineral surfaces. Chem. Geol. 611, 121089.
Suess, E., Balzer, W., Hesse, K.F., Müller, P.J., Ungerer, C.T., Wefer, G., 1982. Calcium carbonate hexahydrate from organic-rich sediments of the Antarctic shelf: precursors of glendonites. Science 216 (4550), 1128–1131.
Sun, E.J., Wu, F.Y., 1998. Along-vein necrosis as indicator symptom on water spinach caused by nickel in water culture. Botan. Bull. Acad. Sinica 39.
Suwa, R., Jayachandran, K., Nguyen, N.T., Boulenouar, A., Fujita, K., Saneoka, H., 2008. Barium toxicity effects in soybean plants. Arch. Environ. Contam. Toxicol. 55 (3), 397–403.
Tlili, M.M., Amor, M.B., Gabrielli, C., Joiret, S., Maurin, G., Rousseau, P., 2002. Characterization of CaCO3 hydrates by micro-Raman spectroscopy. J. Raman Spectrosc. 33 (1), 10–16.
Tollefsen, E., Balic-Zunic, T., Mörth, C.M., et al., 2020. Ikaite nucleation at 35 °C challenges the use of glendonite as a paleotemperature indicator. Sci. Rep. 10, 8141. https://doi.org/10.1038/s41598-020-64751-5.
Ulrich, R., Guillermic, M., Campbell, J., Hakim, A., Han, R., Singh, S., Eagle, R., 2021. Patterns of element incorporation in calcium carbonate biominerals recapitulate phylogeny for a diverse range of marine calcifiers. Front. Earth Sci. 9.
Van Santen, R.A., 1984. The Ostwald step rule. J. Phys. Chem. 88 (24), 5768–5769.
Vickers, M.L., Vickers, M., Rickaby, R.E., Wu, H., Bernasconi, S.M., Ullmann, C.V., Korte, C., 2022. The ikaite to calcite transformation: Implications for palaeoclimate studies. Geochim. Cosmochim. Acta 334, 201–216.
Vosylienė, M.Z., Mikalajūnė, A., 2006. Effect of heavy metal model mixture on rainbow trout biological parameters. Ekologija 4, 12–17.
Wu, S.H., 1994. Effect of manganese excess on the soybean plant cultivated under various growth conditions. J. Plant Nutr. 17 (6), 991–1003.
Xyla, A.G., Koutsoukos, P.G., 1989. Quantitative analysis of calcium carbonate polymorphs by infrared spectroscopy. J. Chem. Soc., Faraday trans. Transactions 1: Phys. Chem. in Condensed Phases 85 (10), 3165–3172.
Zabel, M., Schulz, H.D., 2001. Importance of submarine landslides for non-steady state conditions in pore water systems—lower Congo (Congo) deep-sea fan. Mar. Geol. 176, 87–99.
Zhou, X., Lu, Z., Rickaby, R.E., Domack, E.W., Wellner, J.S., Kennedy, H.A., 2015. Ikaite Abundance Controlled by Porewater Phosphorus Level: potential Links to Dust and Productivity. J. Geodyn. 123, 269–281.
Zmarzly, D.L., Lewin, R.A., 1986. Cation requirements for autotomy or retention of flagellaby the marine alga Tetraselmis subcordiformis (Wille) Hazen (Prasinophyceae, Chlorophyta). Phycologia 25 (4), 575–579.
Zou, Z., Bertinetti, L., Habraken, W.J., Fratzl, P., 2018. Reentrant phase transformation from crystalline ikaite to amorphous calcium carbonate. CrystEngComm 20 (21), 2902–2906.
Zhang, Z., Xie, Y., Xu, X., Pan, H., Tang, R., 2012. Transformation of amorphous calcium carbonate into aragonite. J. Cryst. Growth 343 (1), 62–67.